Electronic Supplementary Information

Supramolecular Fluorescence Enhancement via Coordination-Driven Self-Assembly in bis-Picolylcalixarene Blue-Emitting $M_2L_2X_n$ Macrocycles

Edmundo Guzmán-Percástegui,[a] Mireille Vonlanthen,[b] Beatriz Quiroz-García,[a] Marcos Flores-Alamo,[c] Ernesto Rivera,[b] and Ivan Castillo[a]*

[a]Instituto de Química, [b]Instituto de Investigaciones en Materiales, and [c]Facultad de Química,
Universidad Nacional Autónoma de México, Circuito Exterior, Ciudad Universitaria, México D. F.
04510, México.

Table of Contents

1. Synthesis of metallomacrocycles 1-10

[$Zn_2L_2Cl_4$] (1). To a solution of Zinc chloride (9.0 mg, 0.07 mmol) in acetonitrile was added **L** (50.1 mg, 0.06 mmol) in three portions under N_2 over 20 minutes. The resulting suspension was further stirred at room temperature for 4h, the precipitate was vacuum filtered and washed with cold acetonitrile and cold methanol to give **1** as white solid. Yield: 52 mg, 91%; m.p.: 278-281°C. ^{1}H NMR (400 MHz, $CDCl_3$, 25°C): δ = 8.79 (br, 8H, Py), 8.01 (br, 8H, Py), 7.02 (s, 8H, Ar), 6.91 (br, 4H, OH), 6.76 (s {br}, 8H, Ar), 5.19 (s {br}, 8H, OCH_2–), 4.17 (d, $^2J_{H–H}$ = 13.0 Hz, 8H, –CH_2–), 3.30 (br, 8H, –CH_2–), 1.26 (s, 36H, ^{t}Bu), 0.92 (s {br}, 36H, ^{t}Bu). IR (KBr): ν = 3466m (br) (O─H), [2958s, 2867m] (C─H), 1622m (C═N), [1482s, 1431m] (C═C), 1259m, 1198s, 1028s, 795s. MS (+ESI, CH_3OH): *m/z* = 1897.8 [$\mathbf{Zn_2L_2Cl_4}$–Cl^-]$^+$, 1798.9 [$\mathbf{Zn_2L_2Cl_4}$–Zn^+–$2Cl^-$+H^+]$^+$, 1761.9 [$\mathbf{Zn_2L_2Cl_4}$–Zn^+–$3Cl^-$]$^+$. Elemental analysis calcd (%) for $C_{112}H_{138}Cl_4N_4O_{11}Zn_2$ C 67.64, H 6.99, N 2.82; found C 67.51, H 6.76, N 2.80.

[$Zn_2L_2(NO_3)_4$] (2). Zinc nitrate hexahydrate (58.9 mg, 0.19 mmol) was added to a solution of **L** (150 mg, 0.18 mmol) in methanol. After 6h of vigorous stirring at room temperature, the resulting suspension is vacuum filtered and washed with cold methanol, acetonitrile and hexanes to yield **2** as a white solid. Yield: 152 mg, 83%; m.p. > 300°C. ^{1}H NMR (400 MHz, $CDCl_3$, 25°C): δ = 8.66 (d, $^3J_{H–H}$ = 6.0 Hz, 8H, Py), 8.13 (d, $^3J_{H–H}$ = 5.8 Hz, 8H, Py), 7.18 (s, 4H, OH), 7.08 (s, 8H, Ar), 6.88 (s, 8H, Ar), 5.22 (s, 8H, OCH_2–), 4.23 (d, $^2J_{H–H}$ = 13.1 Hz, 8H, –CH_2–), 3.41 (d, $^2J_{H–H}$ = 13.2 Hz, 8H, –CH_2–), 1.29 (s, 36H, ^{t}Bu), 0.98 (s, 36H, ^{t}Bu). ^{13}C NMR (75 MHz, $CDCl_3$, 25°C): δ = 151.2, 150.3, 149.6, 148.8, 148.1, 142.3, 132.5, 127.4, 126.1, 125.5, 123.3, 75.3, 34.2, 34.0, 31.8, 31.6, 31.1. MS (+ESI, CH_3OH): *m/z* = 1979.1 [$\mathbf{Zn_2L_2(NO_3)_4}$–NO_3^-]$^+$, 1789.2 [$\mathbf{Zn_2L_2(NO_3)_4}$–$4NO_3^-$–$3H^+$]$^+$. IR (KBr): ν = 3448w (br) (O─H), [2956s, 2867w] (C─H), 1622m (C═N), [1481s, 1430m] (C═C), 1291s, 1199s, 1025m, 811s.

Elemental analysis calcd (%) for $C_{112}H_{132}N_8O_{20}Zn_2$ C 65.91, H 6.52, N 5.49; found C 66.72, H 6.71, N 5.41.

$[Zn_2L_2(ClO_4)_4]$ (3). Zinc perchlorate hexahydrate (80.0 mg, 0.22 mmol) was added to a solution of **L** (150 mg, 0.18 mmol) in methanol. After 6h of vigorous stirring at room temperature, the resulting suspension is vacuum filtered and washed with cold methanol and ethanol to give **3** as a white solid. Yield: 166 mg, 84%; m.p. > 300°C. ^1H NMR (400 MHz, $CDCl_3$, 25°C): δ = 8.59 (br, 8H, Py), 7.89 (br, 8H, Py), 7.07 (s, 8H, Ar), 6.80 (s [br], 8H, Ar), 5.13 (s, 8H, OCH_2–), 4.22 (d, $^2J_{H–H}$ = 13.0 Hz, 8H, –CH_2–), 3.34 (d, $^2J_{H–H}$ = 13.0 Hz, 8H, –CH_2–), 1.29 (s, 36H, ^{t}Bu), 0.94 (s, 36H, ^{t}Bu). MS (+ESI, CH_3OH): *m/z* = 2089.2 [$\mathbf{Zn_2L_2(ClO_4)_4}$–$ClO_4^-$]$^+$, 1824.4 [$\mathbf{Zn_2L_2(ClO_4)_4}$–$Zn^+$–$3ClO_4^-$]$^+$. IR (KBr): ν = 3451w (br) (O─H), [2955m, 2867w] (C─H), 1622w (C═N), [1482s, 1433m] (C═C), 1196m, 1098s, 1031s, 811s. Elemental analysis calcd (%) for $C_{114}H_{138}Cl_4N_4O_{25}Zn_2$ C 61.21, H 6.22, N 2.50; found C 61.35, H 6.94, N 2.41.

$[Pd_2Cl_4L_2]$ (4). Palladium chloride (46.8 mg, 0.26 mmol) was refluxed in dry acetonitrile (20 mL) for 1h. After cooling to room temperature **L** (200 mg, 0.24 mmol) was added to the yellow solution in portions over 20 minutes under N_2 and the orange solution was refluxed for 4h. The final yellow suspension was filtered and the solid was washed with hot acetonitrile and diethyl ether yielding macrocycle **4** as a pale yellow solid. Yield: 210 mg, 83%; m.p. > 300°C. ^1H NMR (400 MHz, $CDCl_3$, 25°C): δ = 9.00 (d, $^3J_{H–H}$ = 6.7 Hz, 8H, Py), 7.76 (d, $^3J_{H–H}$ = 6.7 Hz, 8H, Py), 7.08 (s, 8H, Ar), 6.80 (s, 4H, OH), 6.78 (s, 8H, Ar), 5.14 (s, 8H, OCH_2–), 4.17 (d, $^2J_{H–H}$ = 13.1 Hz, 8H, –CH_2–), 3.35 (d, $^2J_{H–H}$ = 13.2 Hz, 8H, –CH_2–), 1.31 (s, 36H, ^{t}Bu), 0.91 (s, 36H, ^{t}Bu). ^{13}C NMR (75 MHz, $CDCl_3$, 25°C): δ = 153.7, 150.2, 149.6, 148.8, 147.8, 141.9, 132.0, 127.3, 125.7, 125.0, 121.3, 74.9, 34.1, 34.0, 31.9, 31.5, 31.0. MS (+ESI, CH_2Cl_2): *m/z* = 1981.2 [$\mathbf{Pd_2Cl_4L_2}$–Cl^-]$^+$, 1803.4 [$\mathbf{Pd_2Cl_4L_2}$–Pd^+–$3Cl^-$]$^+$. IR (KBr): ν =

3433w (br) (O─H), [2955s, 2904w, 2866w] (C─H), 1621m (C═N), [1482s, 1429m] (C═C), 1194s, 1022m, 814s. Elemental analysis calcd (%) for $C_{112}H_{136}Cl_4N_4O_{10}Pd_2$ C 65.53, H 6.68, N 2.73; found C 65.68, H 6.71, N 2.77.

[Ag$_2$L$_2$(BF$_4$)$_2$] (5). To a solution of silver tetrafluoroborate (24.6 mg, 0.13 mmol) in acetonitrile (10 mL) **L** ligand (100 mg, 0.12 mmol) was added in portions over 20 minutes under N_2. The resulting suspension was sonicated for ten minutes, further stirred for 6h at room temperature and protected from light. The solvent was allowed to slowly evaporate away from light and the precipitate was washed with cold ethanol and acetonitrile, compound **5** was recovered as a brownish solid. Yield: 116 mg, 90%; m.p.: 243-246°C. ^{1}H NMR (400 MHz, $CDCl_3$, 25°C): δ = 8.63 (d, $^3J_{H–H}$ = 5.6 Hz, 8H, Py), 8.04 (d, $^3J_{H–H}$ = 5.6 Hz, 8H, Py), 7.49 (s, OH, 4H), 7.08 (s, 8H, Ar), 6.92 (s, 8H, Ar), 5.12 (s, 8H, OCH_2–), 4.27 (d, $^2J_{H–H}$ = 13.0 Hz, 8H, –CH_2–), 3.43 (d, $^2J_{H–H}$ = 13.0 Hz, 8H, –CH_2–), 1.28 (s, 36H, ^{t}Bu), 1.02 (s, 36H, ^{t}Bu). ^{13}C NMR (75 MHz, $CDCl_3$, 25°C): δ = 152.6, 150.4, 150.1, 148.9, 148.2, 142.3, 132.7, 127.3, 126.1, 125.4, 122.9, 75.5, 34.2, 34.0, 31.9, 31.8, 31.1. MS (+ESI, CH_3CN): *m/z* = 1964.1 $[\mathbf{Ag_2L_2(BF_4)_2}–(BF_4)^-]^+$, 1769.9 $[\mathbf{Ag_2L_2(BF_4)_2}–Ag^+–2(BF_4)^-]^+$, 939.0 $[\mathbf{Ag_2L_2(BF_4)_2}–(AgL)^+–2(BF_4)^-]^+$. IR (KBr): ν = 3373m (br) (O─H), [2958w, 2868w] (C─H), 1615m (C═N), [1482m, 1428w] (C═C), 1197m, 1023s, 809m. Elemental analysis calcd (%) for $C_{112}H_{134}Ag_2B_2F_8N_4O_9$ C 65.00, H 6.53, N 2.71; found C 65.03, H 6.68, N 2.74.

[Ag$_2$L$_2$(CF$_3$SO$_3$)$_2$] (6). Complex **6** was prepared in a similar procedure to that employed for **5**. To a solution of $AgCF_3SO_3$ (34.2 mg, 0.13 mmol) in dry acetonitrile (10 mL) **L** ligand (100 mg, 0.12 mmol) was added in portions (5) over 30 minutes under nitrogen flow. Compound **6** was recovered as a white solid. Yield: 114 mg, 89%; m.p.: 266-270°C. ^{1}H NMR (400 MHz, $CDCl_3$, 25°C): δ = 8.70 (d, $^3J_{H–H}$ = 5.9 Hz, 8H, Py), 7.92 (d, $^3J_{H–H}$ = 6.4 Hz, 8H, Py), 7.31 (s, OH, 4H), 7.11 (s, 8H, Ar), 6.89 (s, 8H, Ar), 5.12 (s, 8H, OCH_2–), 4.30 (d, $^2J_{H–H}$ = 10.7 Hz, 8H, –CH_2–), 3.43 (d, $^2J_{H–H}$ = 13.2 Hz, 8H, –CH_2–), 1.31 (s, 36H, ^{t}Bu), 0.99 (s, 36H, ^{t}Bu). ^{13}C NMR (75 MHz, $CDCl_3$, 25°C): δ = 152.6, 150.5, 149.3, 148.9, 148.2, 142.2, 132.6, 127.3, 126.0, 125.3, 122.6, 75.6, 34.2, 34.0, 31.8, 31.7, 31.2. MS (+ESI, CH_3CN): *m/z* = 2283.6 [$\mathbf{Ag_2L_2(CF_3SO_3)_2}$+$Ag^+$]$^+$, 2025.8 [$\mathbf{Ag_2L_2(CF_3SO_3)_2}$–$(CF_3SO_3)^-$]$^+$, 1769.9 [$\mathbf{Ag_2L_2(CF_3SO_3)_2}$–$Ag^+$–$2(CF_3SO_3)^-$]$^+$, 939.3 [$\mathbf{Ag_2L_2(CF_3SO_3)_2}$–$(AgL)^+$–$2(CF_3SO_3)^-$]$^+$. IR (KBr): ν = 3368m (br) (O─H), [2959s, 2868w] (C─H), 1616w (C═N), [1481m, 1428w] (C═C), 1229s, 1023s, 807m. Elemental analysis calcd (%) for $C_{114}H_{136}Ag_2F_6N_4O_{16}S_2$ C 61.89, H 6.20, N 2.53; found C 61.84, H 6.35, N 2.55.

[$Ag_2L_2(PF_6)_2$] (7). Complex **7** was prepared in a similar procedure to that employed for **5**. To a solution of $AgPF_6$ (34.2 mg, 0.13 mmol) in dry acetonitrile (10 mL) **L** ligand (100 mg, 0.12 mmol) was added in portions (5) over 30 minutes under nitrogen flow. The white suspension was filtered and the solid was washed with cold acetonitrile. Compound **7** was recovered as a yellowish solid. Yield: 91 mg, 92%; m.p.: 257-260°C. ^{1}H NMR (400 MHz, $CDCl_3$, 25°C): δ = 8.60 (d, $^3J_{H–H}$ = 5.8 Hz, 8H, Py), 8.01 (d, $^3J_{H–H}$ = 5.7 Hz, 8H, Py), 7.25 (s, OH, 4H), 7.09 (s, 8H, Ar), 6.87 (s, 8H, Ar), 5.16 (s, 8H, OCH_2–), 4.25 (d, $^2J_{H–H}$ = 13.0 Hz, 8H, –CH_2–), 3.39 (d, $^2J_{H–H}$ = 13.0 Hz, 8H, –CH_2–), 1.30 (s, 36H, ^{t}Bu), 0.98 (s, 36H, ^{t}Bu). ^{13}C NMR (75 MHz, $CDCl_3$, 25°C): δ = 152.3, 150.3, 150.2, 148.7, 147.9, 142.1, 132.3, 127.3, 125.8, 125.2, 122.2, 74.9, 34.0, 33.9, 31.7, 31.5, 31.0. MS (+ESI, CH_3CN): *m/z* = 2022.8 [$\mathbf{Ag_2L_2(PF_6)_2}$–$(PF_6)^-$]$^+$, 1769.9 [$\mathbf{Ag_2L_2(PF_6)_2}$–Ag^+–$2(PF_6)^-$]$^+$, 939.4 [$\mathbf{Ag_2L_2(PF_6)_2}$–$(AgL)^+$–$2(PF_6)^-$]$^+$. IR (KBr): ν = [2957m, 2869w] (C─H), 1619w (C═N), [1482m, 1438w] (C═C), 1197m, 1027w, 839s. Elemental analysis calcd (%) for $C_{112}H_{134}Ag_2F_{12}N_4O_9P_2$ C 61.54, H 6.18, N 2.56; found C 61.84, H 6.20, N 2.52.

[$Ag_2L_2(SbF_6)_2$] (8). Complex **8** was prepared in a similar procedure to that employed for **5**. To a solution of $AgSbF_6$ (43.4 mg, 0.13 mmol) in dry acetonitrile (10 mL) **L** (100 mg, 0.12 mmol) was added in 5 portions over 30 minutes under nitrogen flow. The suspension was filtered and the solid was washed with cold acetonitrile. Compound **8** was recovered as a yellowish solid. Yield: 126 mg, 90%; m.p.: 226-230°C. ^{1}H NMR (400 MHz, $CDCl_3$, 25°C): δ = 8.54 (d, $^3J_{H\text{–}H}$ = 5.9 Hz, 8H, Py), 8.03 (d, $^3J_{H\text{–}H}$ = 6.4 Hz, 8H, Py), 7.25 (s, OH, 4H), 7.06 (s, 8H, Ar), 6.85 (s, 8H, Ar), 5.13 (s, 8H, OCH_2–), 4.21 (d, $^2J_{H\text{–}H}$ = 10.7 Hz, 8H, –CH_2–), 3.33 (d, $^2J_{H\text{–}H}$ = 13.2 Hz, 8H, –CH_2–), 1.28 (s, 36H, ^{t}Bu), 0.97 (s, 36H, ^{t}Bu). ^{13}C NMR (75 MHz, $CDCl_3$, 25°C): δ = 150.3, 149.0, 147.9, 146.6, 142.1, 132.2, 127.4, 125.8, 125.2, 122.5, 75.5, 34.0, 33.9, 31.7, 31.5, 30.9. MS (+ESI, CH_3CN): *m/z* = 2110.7 [$\mathbf{Ag_2L_2(SbF_6)_2}$–$(SbF_6)^-]^+$, 1769.1 [$\mathbf{Ag_2L_2(SbF_6)_2}$–$Ag^+$–$2(SbF_6)^-]^+$, 938.9 [$\mathbf{Ag_2L_2(SbF_6)_2}$–$(AgL)^+$–$2(SbF_6)^-]^+$. IR (KBr): ν = 3452w (br) (O─H), [2957m, 2866w] (C─H), 1618w (C═N), [1482m, 1431w] (C═C), 1196s, 1028m, 811m, 659s. Elemental analysis calcd (%) for $C_{112}H_{140}Ag_2F_{12}N_4O_{12}Sb_2$ C 55.97, H 5.79, N 2.33; found C 55.55, H 5.69, N 2.35.

[$Cd_2L_2(NO_3)_4$] (9). Cadmium nitrate trihydrate (81.6 mg, 0.26 mmol) was added to a solution of **L** (200 mg, 0.24 mmol) in methanol. After 6h of vigorous stirring at room temperature, the resulting suspension is vacuum filtered and washed with cold methanol and hexanes to yield **9** as a white solid. Yield: 187 mg, 73%; m.p.: 281-285°C. ^{1}H NMR (400 MHz, $CDCl_3$, 25°C): δ = 8.59 (d, $^3J_{H\text{–}H}$ = 5.3 Hz, 8H, Py), 7.99 (d, $^3J_{H\text{–}H}$ = 5.2 Hz, 8H, Py), 7.13 (s, 4H, OH), 7.08 (s, 8H, Ar), 6.84 (s, 8H, Ar), 5.17 (s, 8H, OCH_2–), 4.22 (d, $^2J_{H\text{–}H}$ = 11.8 Hz, 8H, –CH_2–), 3.38 (d, $^2J_{H\text{–}H}$ = 11.2 Hz, 8H, –CH_2–), 1.29 (s, 36H, ^{t}Bu), 0.95 (s, 36H, ^{t}Bu). ^{13}C NMR (75 MHz, $CDCl_3$, 25°C): δ = 150.8, 150.2, 149.6, 148.7, 148.0, 142.0, 132.2, 127.2, 125.8, 125.1, 122.5, 75.0, 33.9, 33.8, 31.8, 31.6, 31.1. MS (+ESI, CH_3OH): *m/z* = 2072.1 [$\mathbf{Cd_2L_2(NO_3)_4}$–$NO_3^-]^+$, 1836.4 [$\mathbf{Cd_2L_2(NO_3)_4}$–Cd^+–$3(NO_3)^-]^+$. IR (KBr): ν = 3358w (br) (O─H), [2958m, 2869w] (C─H), 1618m (C═N), [1482s, 1429s] (C═C), 1296s, 1199s, 813s. Elemental analysis calcd (%) for Elemental analysis calcd (%) for $C_{112}H_{132}Cd_2N_8O_{20}$ C 63.00, H 6.23, N 5.25; found C 63.72, H 6.48, N 5.10.

[$Cd_2L_2(ClO_4)_4$] (10). Cadmium perchlorate hexahydrate (91.0 mg, 0.22 mmol) was added to a solution of **L** (150 mg, 0.18 mmol) in methanol. After 6h of vigorous stirring at room temperature, the resulting suspension is vacuum filtered and washed with cold methanol and ethanol to give **10** as a white solid. Yield: 154 mg, 75%; m.p.: 231-235°C. ^{1}H NMR (400 MHz, $CDCl_3$, 25°C): δ = 8.82 (d [br], 4H, Py), 8.61 (d [br], 4H, Py), 7.94 (d [br], 4H, Py), 7.84 (d [br], 4H, Py), 7.11 (s, 8H, Ar), 6.75–6.67 (m, 12H, Ar, OH), 5.20 (s, 8H, OCH_2–), 4.12 (d, $^2J_{H–H}$ = 12.9 Hz, 8H, –CH_2–), 3.33 (d, $^2J_{H–H}$ = 12.8 Hz, 8H, –CH_2–), 1.31 (s, 36H, ^{t}Bu), 0.87 (s, 36H, ^{t}Bu). MS (+ESI, CH_3OH): *m/z* = 1874.1 [$\mathbf{Cd_2L_2(ClO_4)_4}$–$Cd^+$–$3ClO_4^-$]$^+$, 1810.2 [$\mathbf{Cd_2L_2(ClO_4)_4}$+$2H_2O$–$Cd^+$–$H^+$–$4(ClO_4)^-$]$^+$. IR (KBr): ν = 3498w (br) (O–H), [2956s, 2867m] (C–H), 1617m (C=N), [1481s, 1425m] (C=C), 1199s, 1110s, 1018s, 808s. Elemental analysis calcd (%) for $C_{114}H_{138}Cd_2Cl_4N_4O_{25}$ C 58.74, H 6.00, N 2.40; found C 59.11, H 6.12, N 2.39.

2. IR Spectra

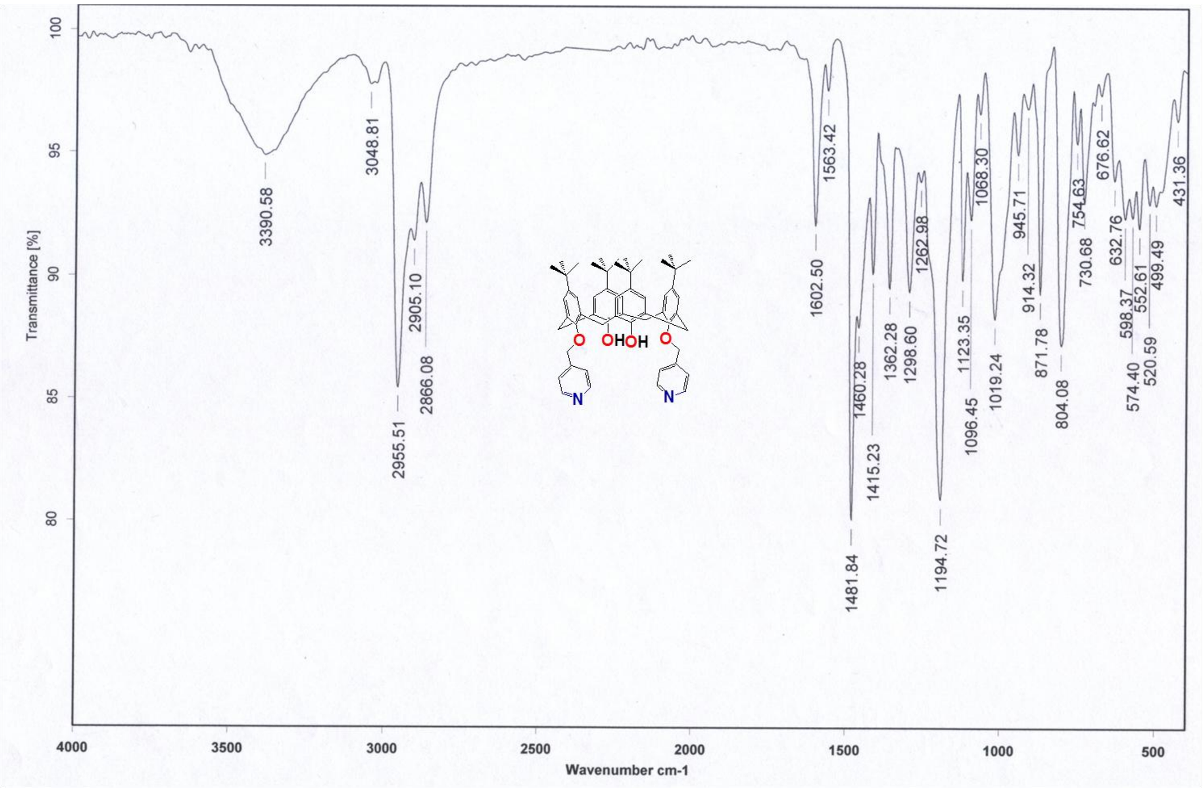

Figure S1. IR spectrum of calix[4]arene **L** in KBr.

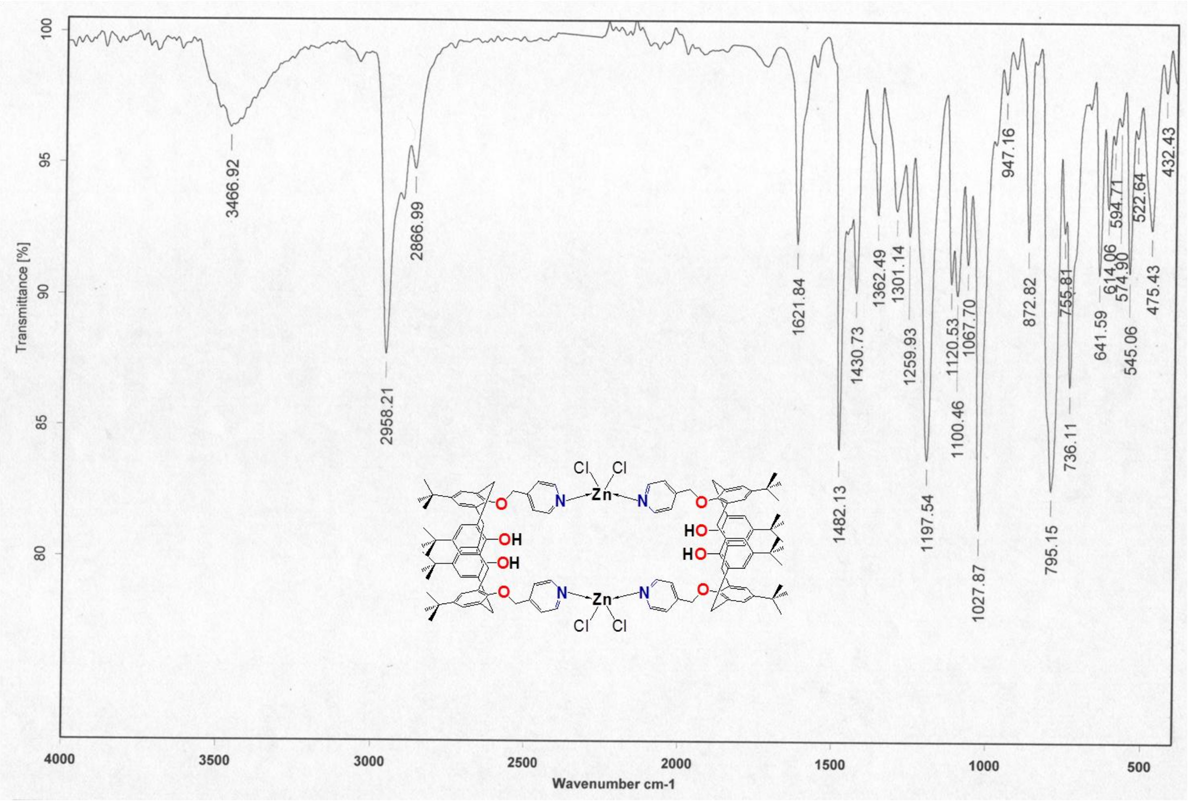

Figure S2. IR spectrum of metallacycle **1** in KBr.

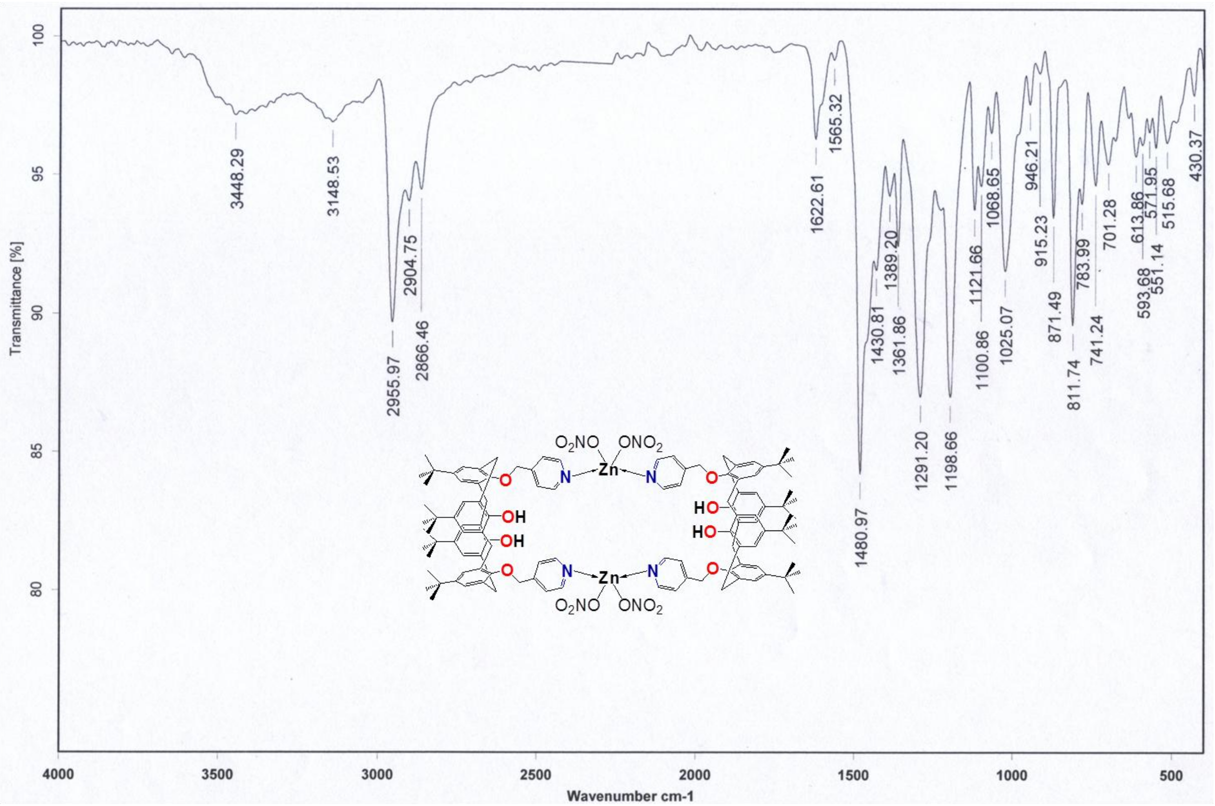

Figure S3. IR spectrum of metallacycle **2** in KBr.

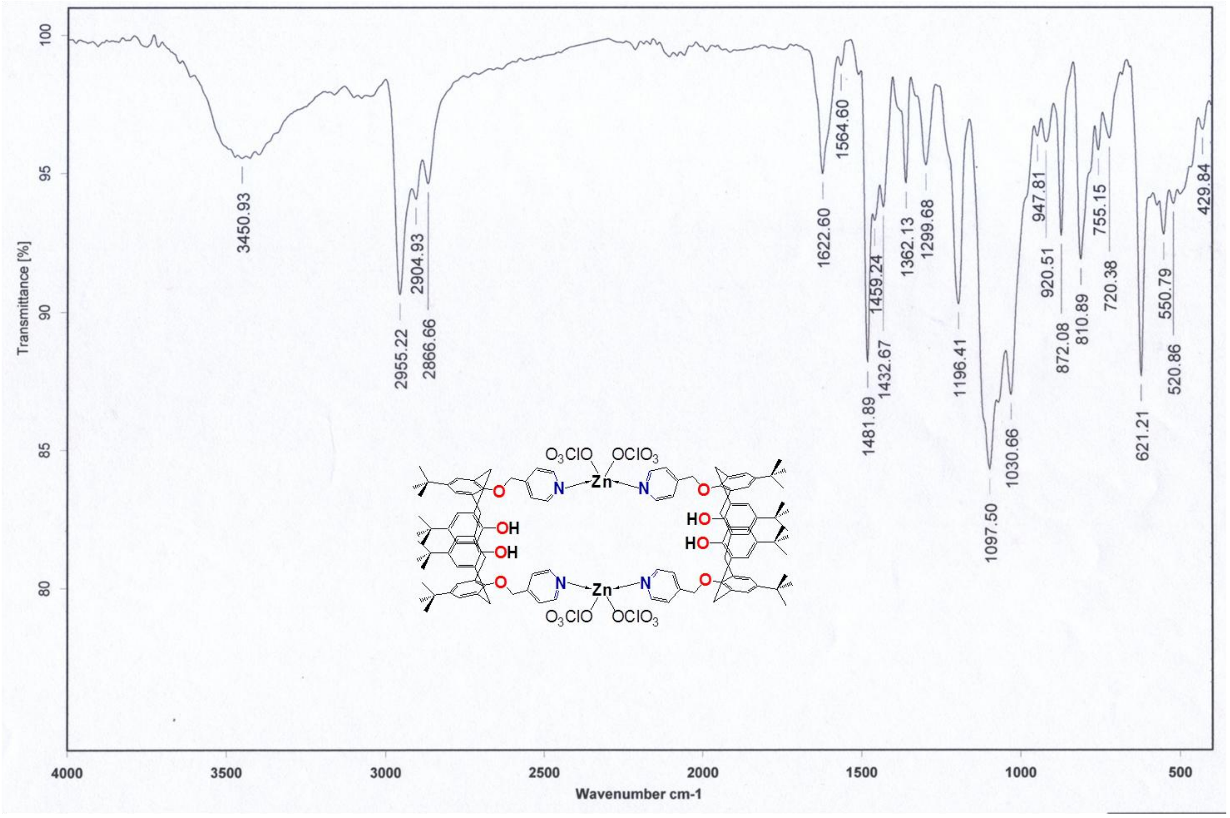

Figure S4. IR spectrum of metallacycle **3** in KBr.

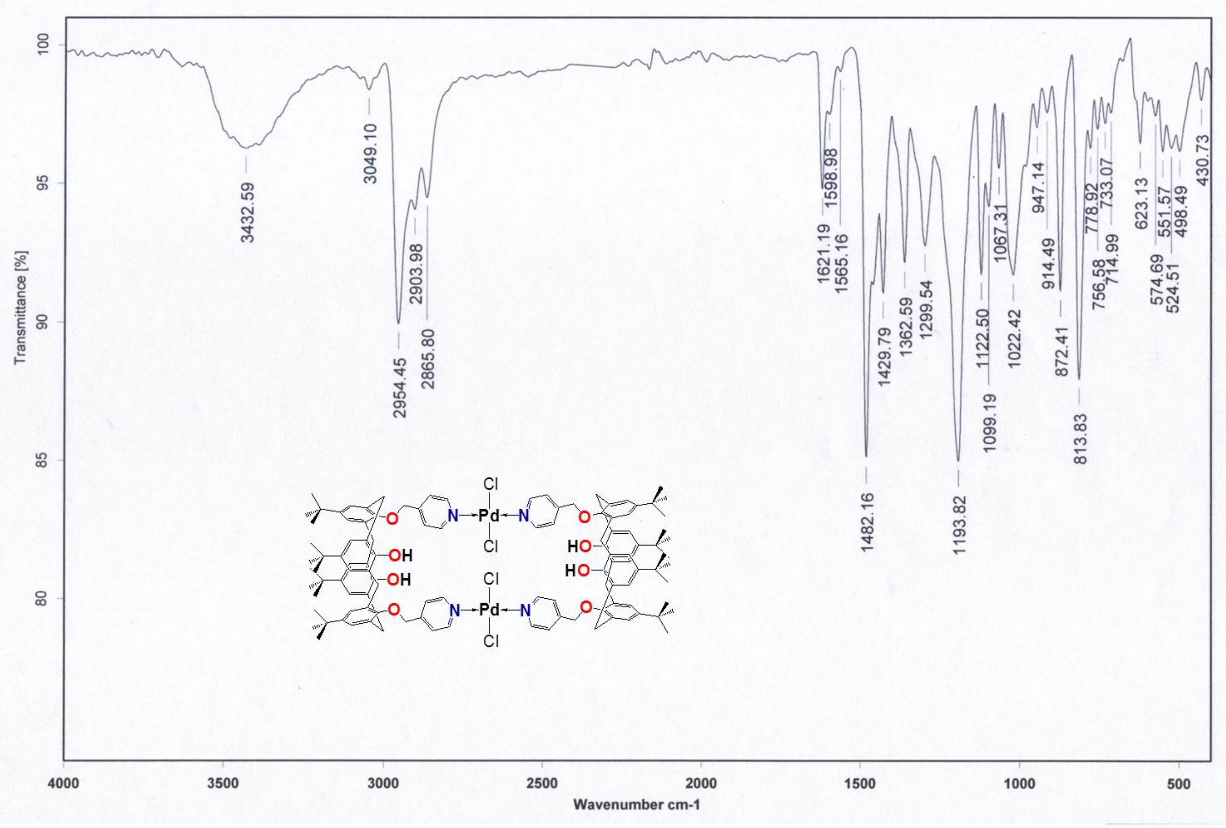

Figure S5. IR spectrum of metallacycle **4** in KBr.

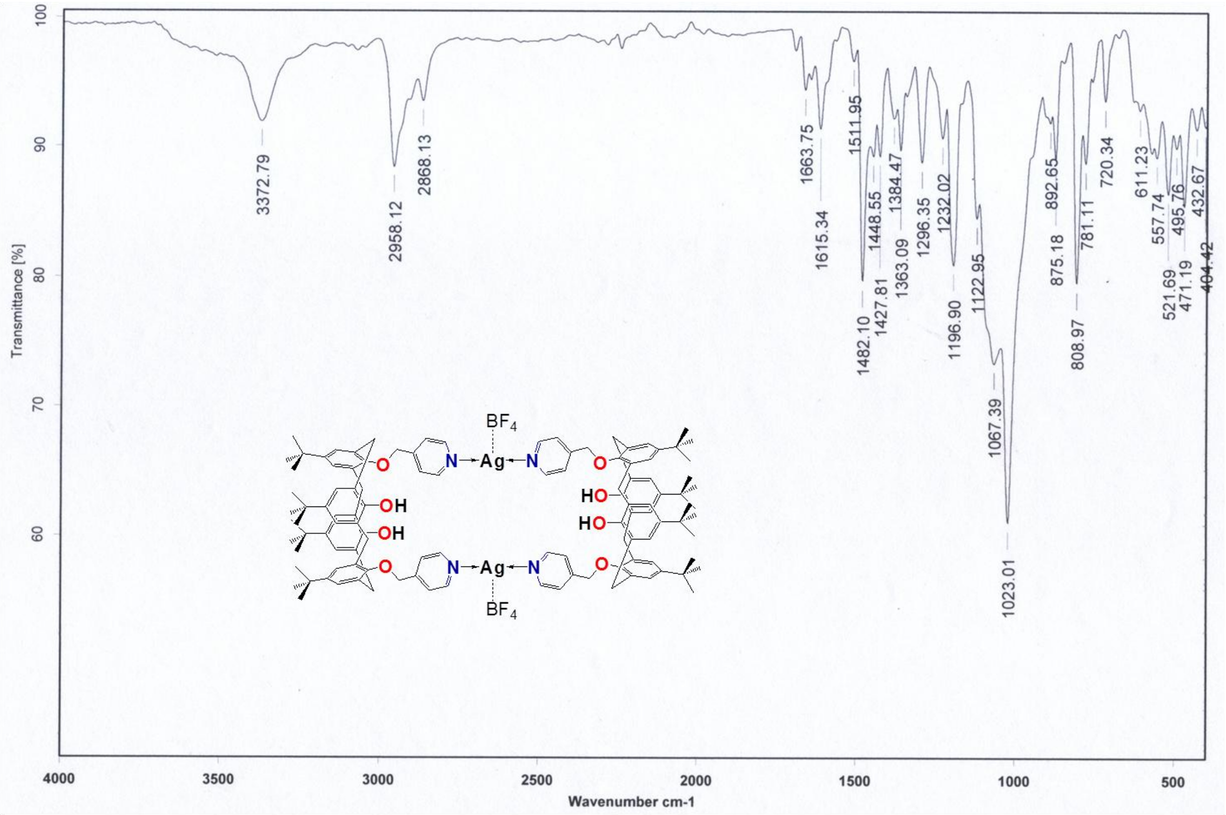

Figure S6. IR spectrum of metallacycle **5** in KBr.

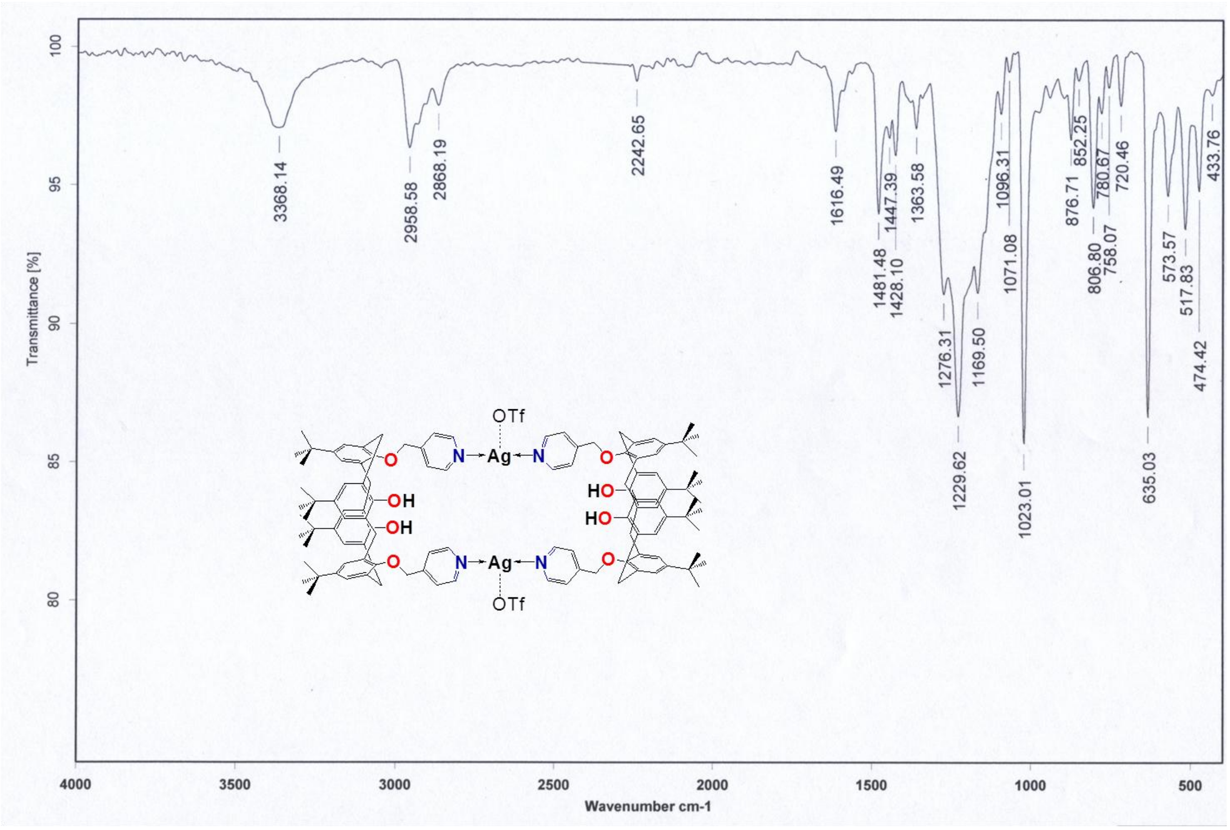

Figure S7. IR spectrum of metallacycle **6** in KBr.

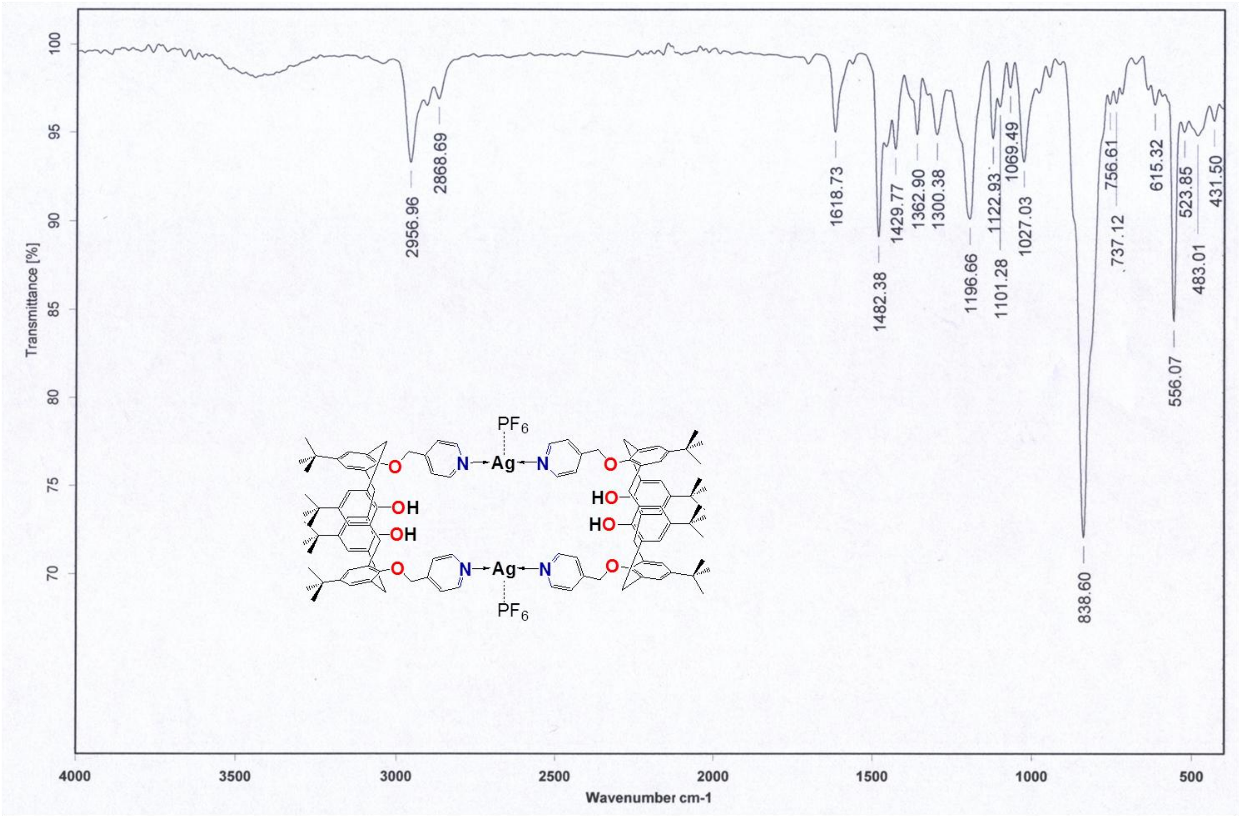

Figure S8. IR spectrum of metallacycle **7** in KBr.

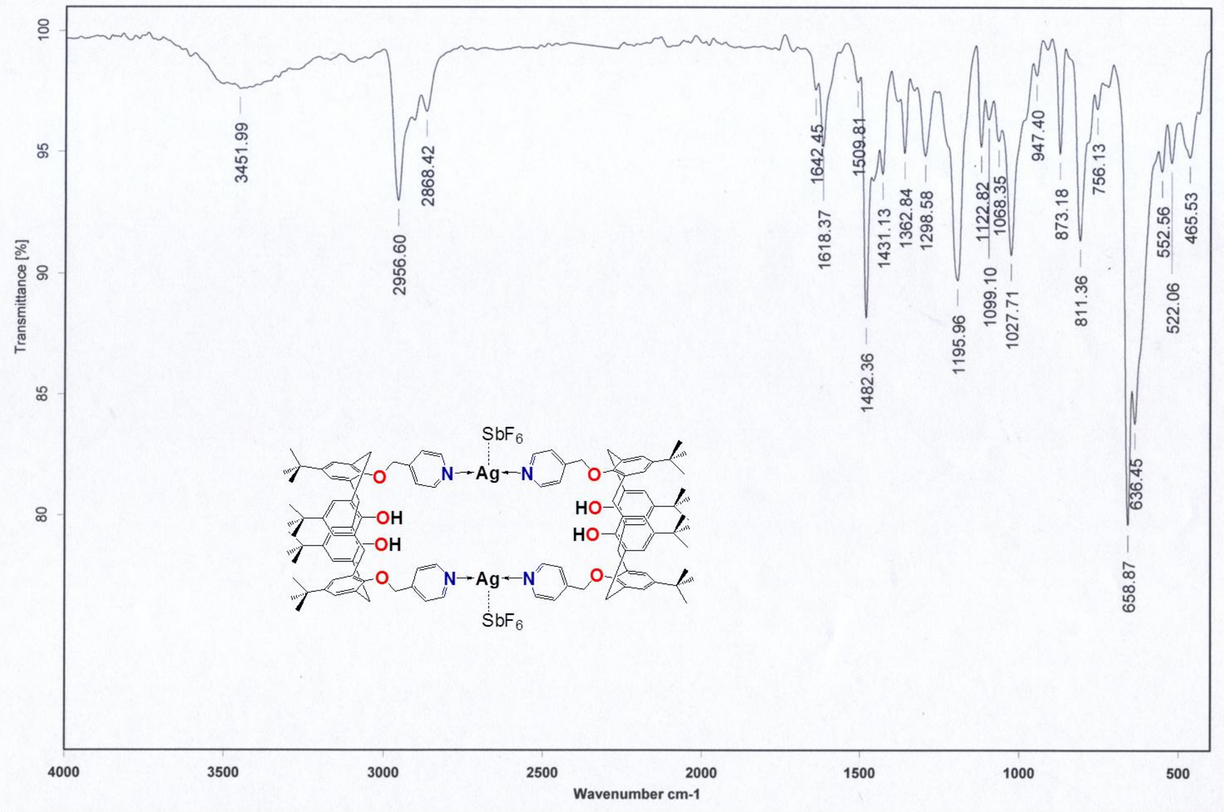

Figure S9. IR spectrum of metallacycle **8** in KBr.

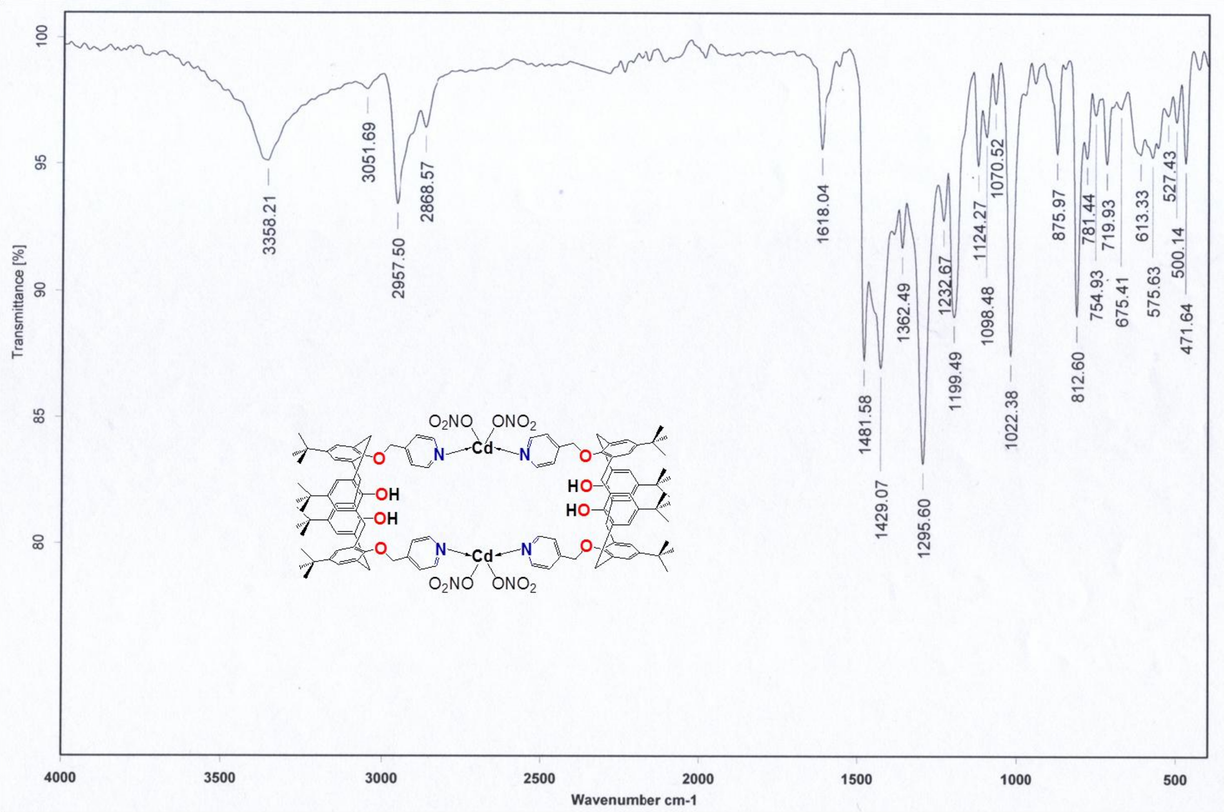

Figure S10. IR spectrum of metallacycle **9** in KBr.

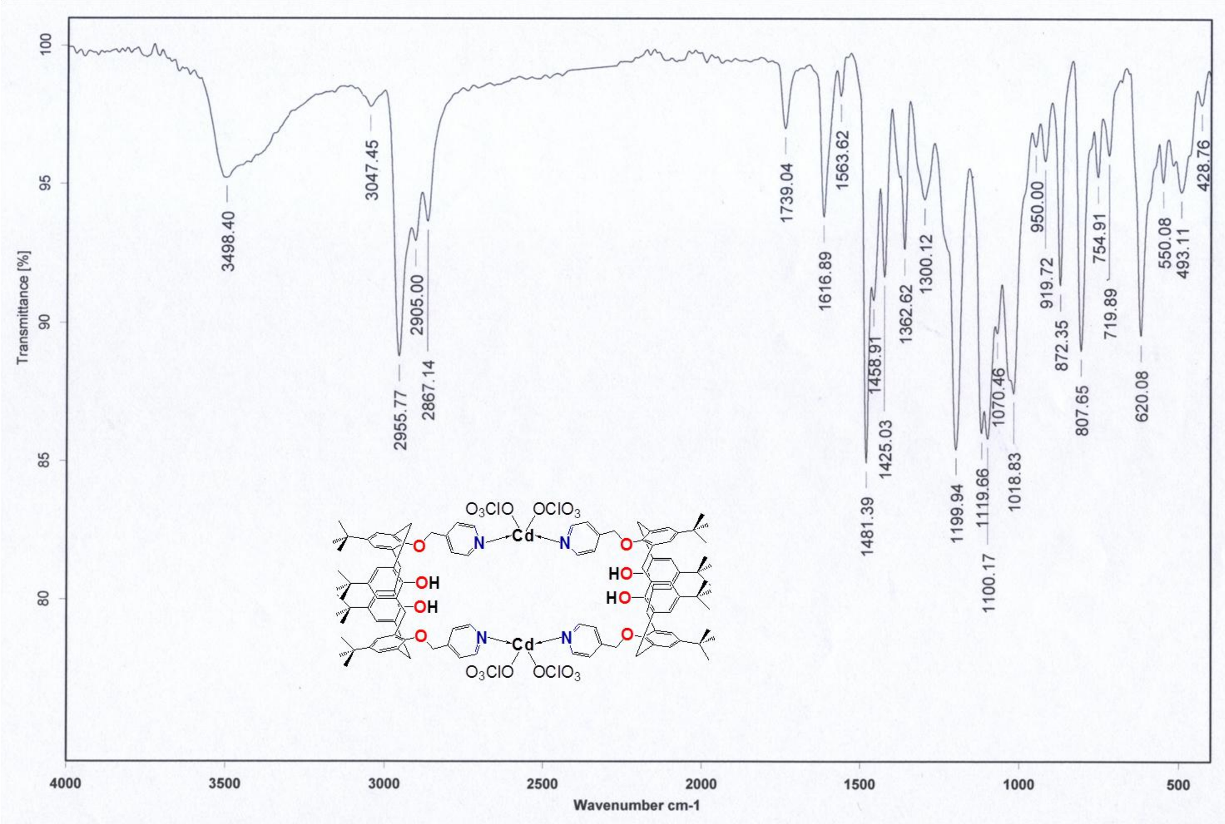

Figure S11. IR spectrum of metallacycle **10** in KBr.

3. ^{1}H and 2D-DOSY NMR Spectra

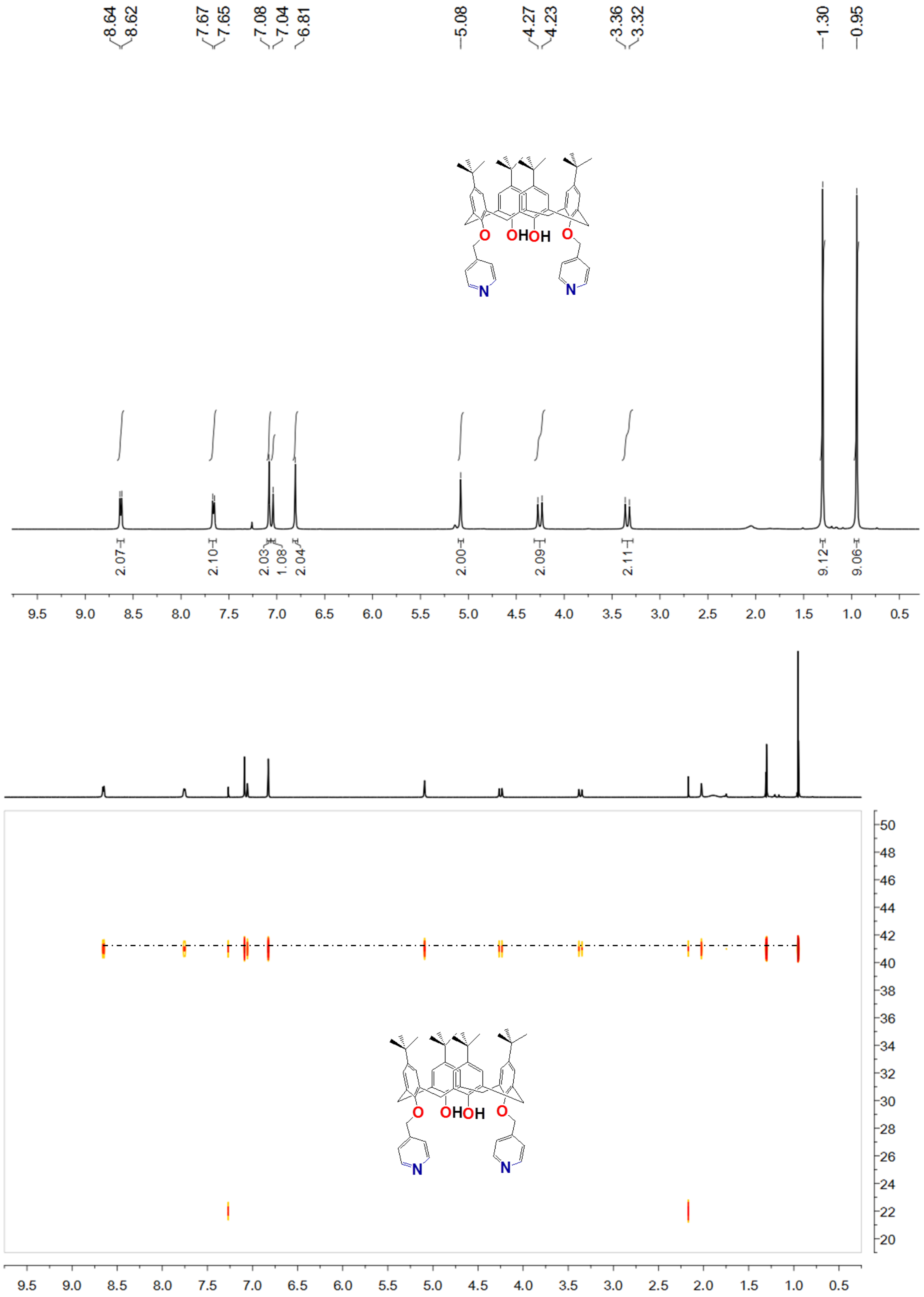

Figure S12. ^{1}H (*top*) and 2D–DOSY (*bottom*) NMR spectra of calix[4]arene **L** in $CDCl_3$ at 25°C.

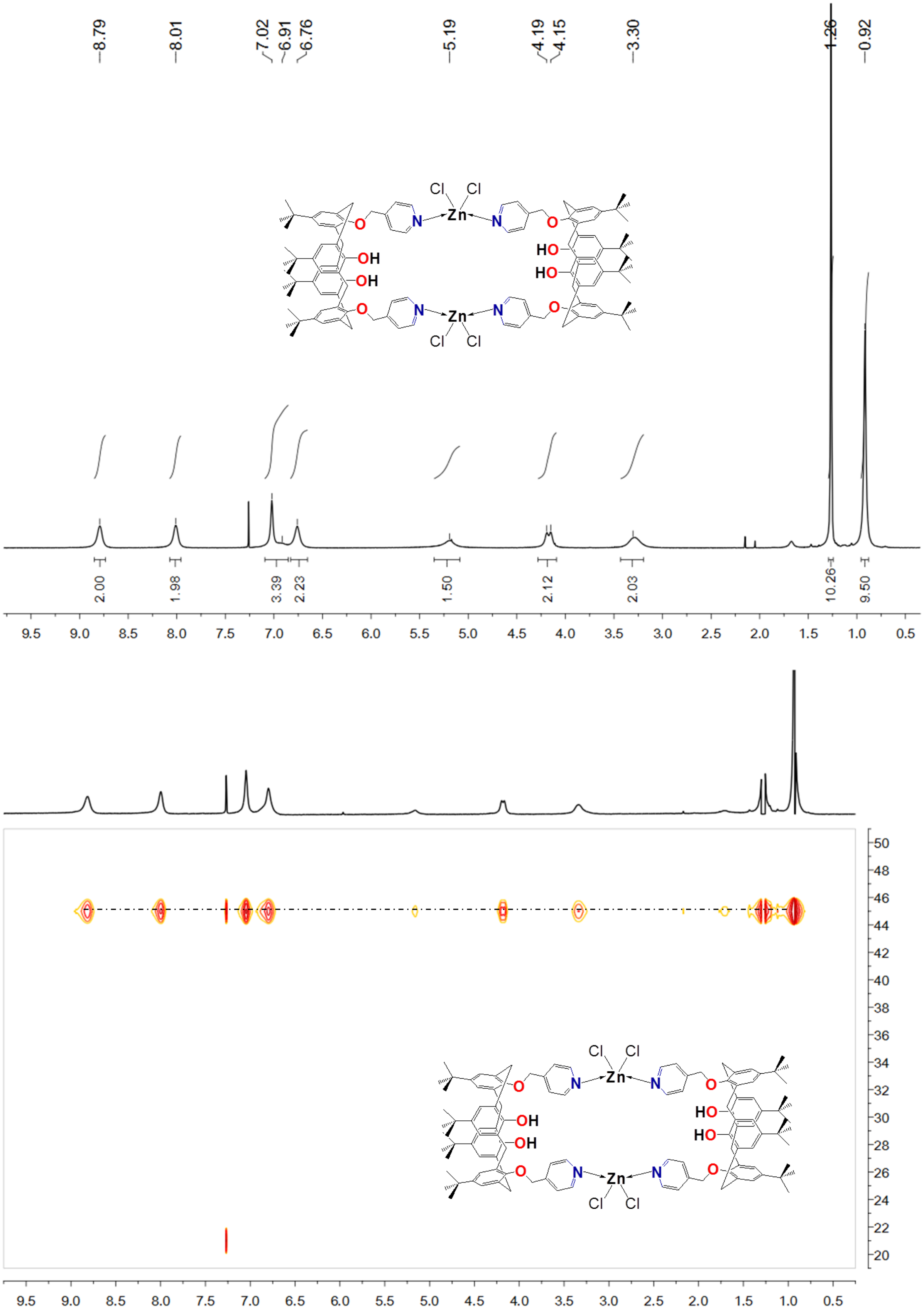

Figure S13. ^{1}H (*top*) and 2D–DOSY (*bottom*) NMR spectra of macrocycle **1** in $CDCl_3$ at 25°C.

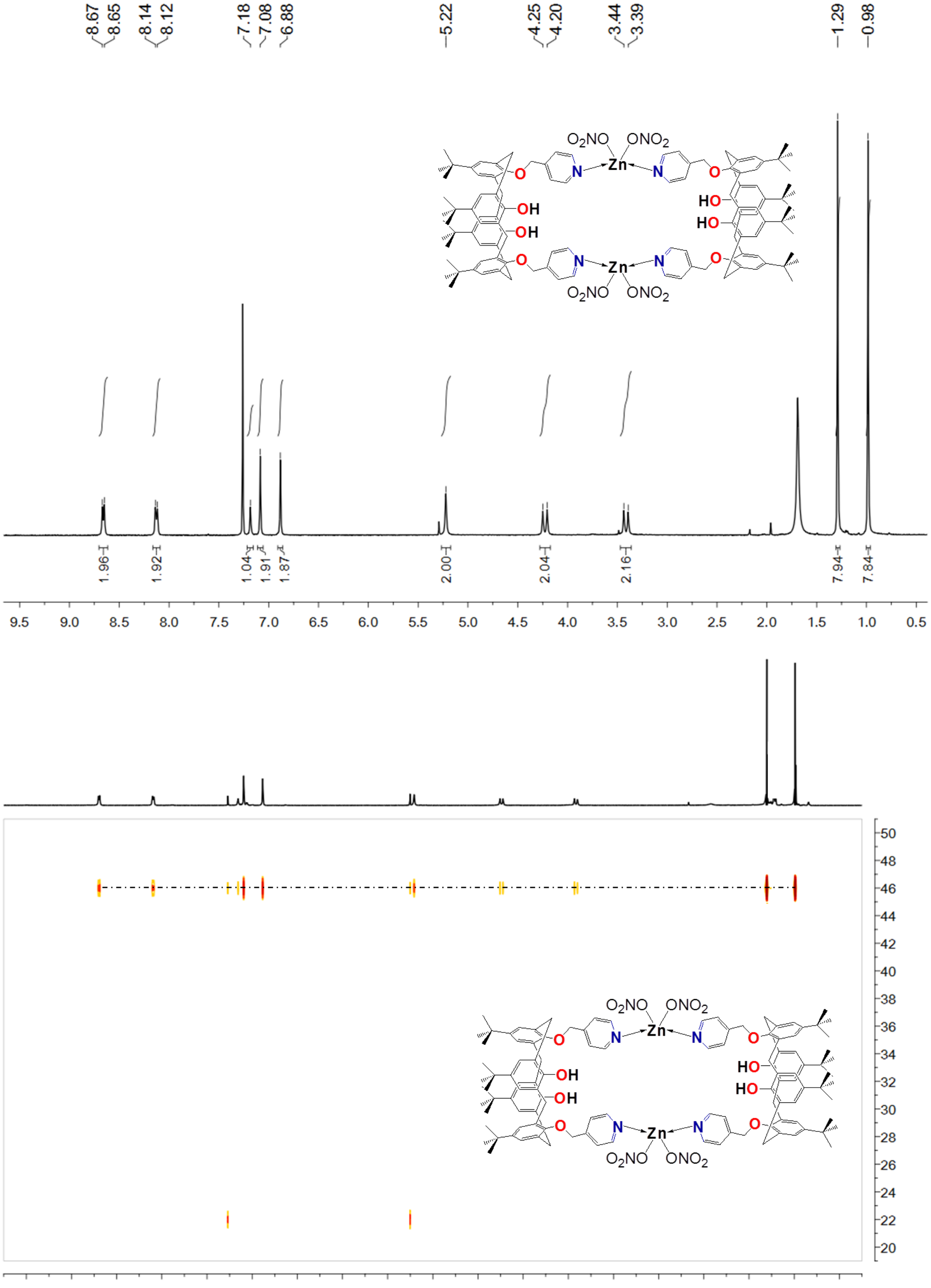

Figure S14. ^{1}H (*top*) and 2D–DOSY (*bottom*) NMR spectra of macrocycle **2** in $CDCl_3$ at 25°C.

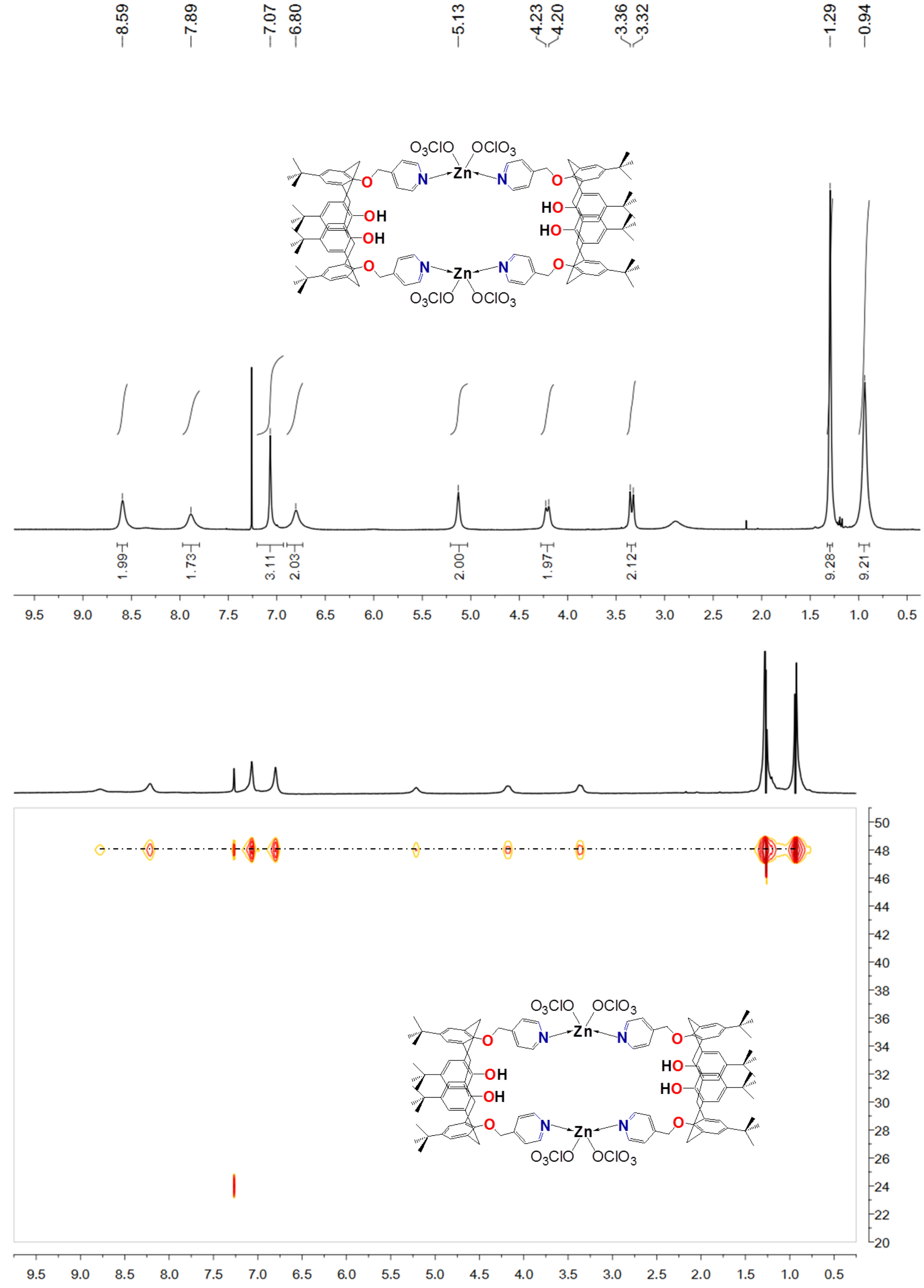

Figure S15. ^{1}H (*top*) and 2D–DOSY (*bottom*) NMR spectra of macrocycle **3** in $CDCl_3$ at 25°C.

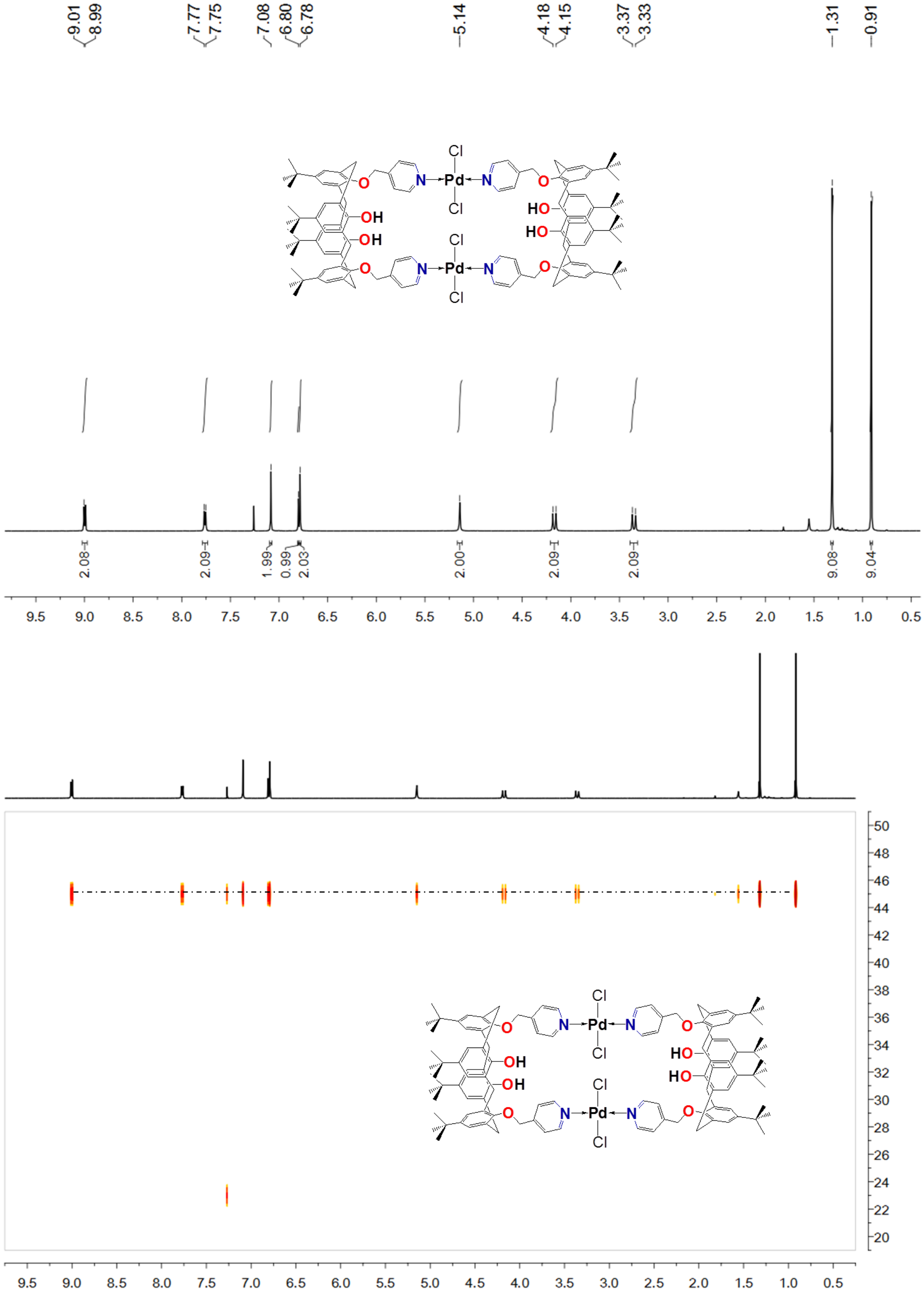

Figure S16. ^{1}H (*top*) and 2D–DOSY (*bottom*) NMR spectra of macrocycle **4** in $CDCl_3$ at 25°C.

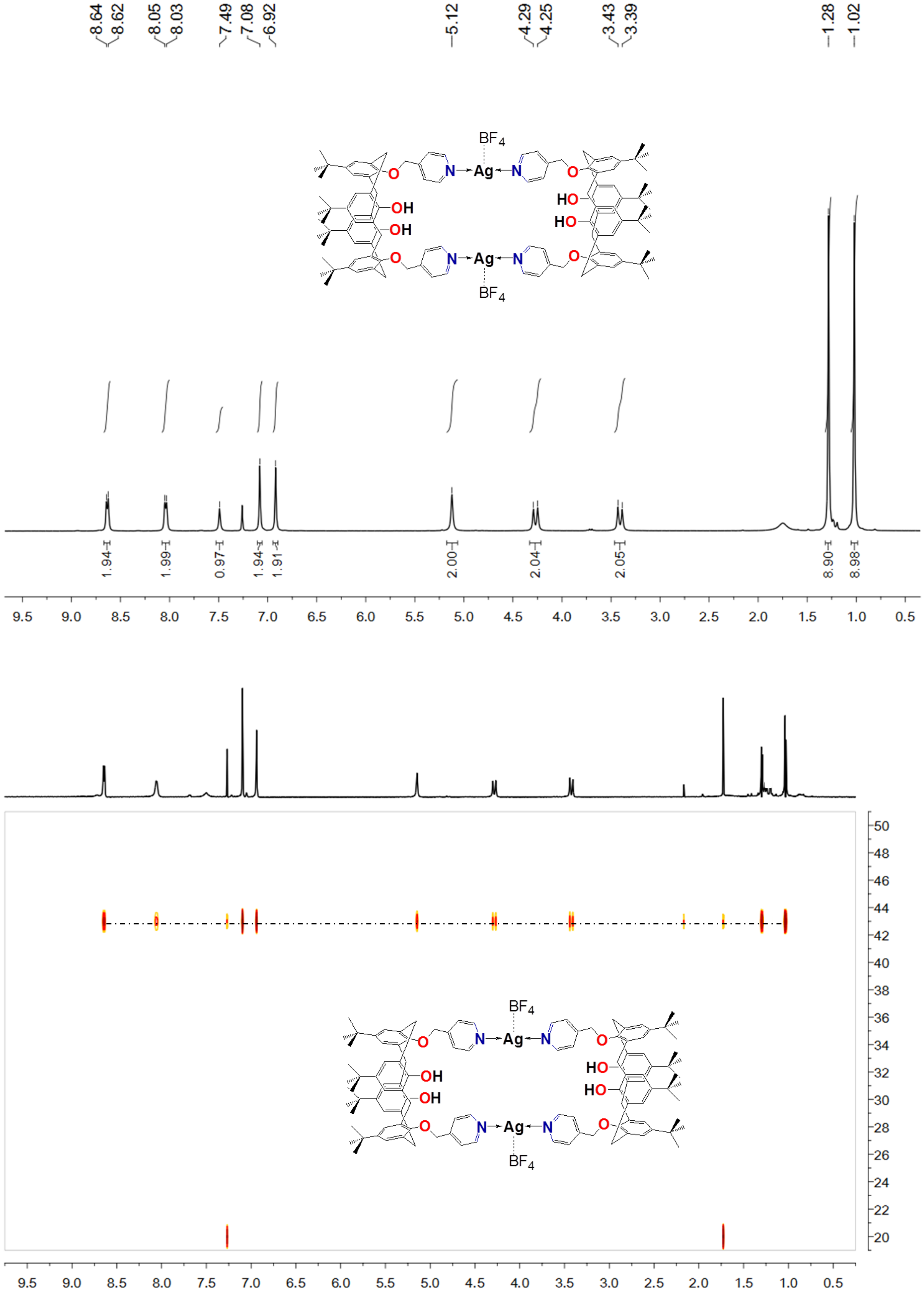

Figure S17. ^{1}H (*top*) and 2D–DOSY (*bottom*) NMR spectra of macrocycle **5** in $CDCl_3$ at 25°C.

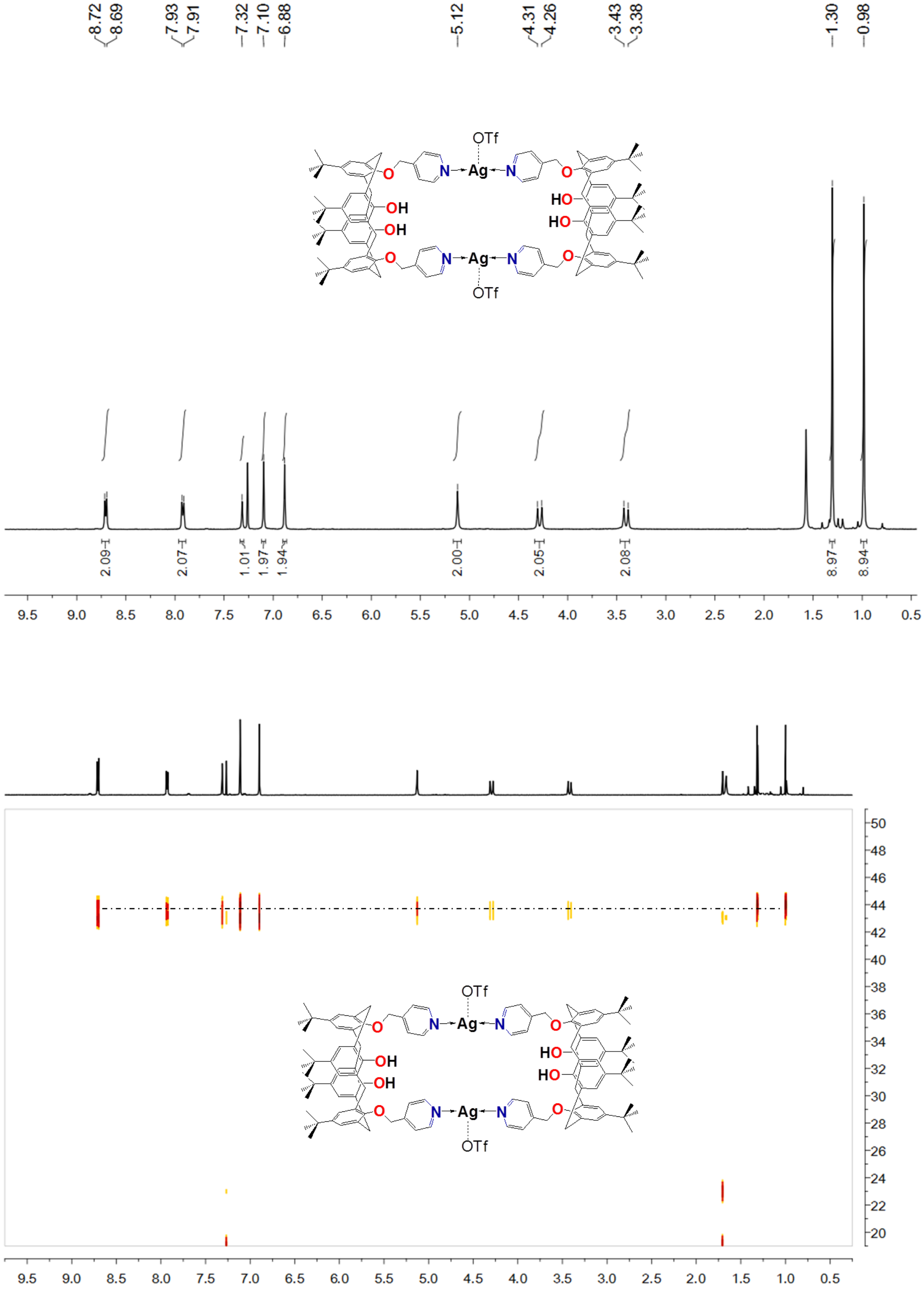

Figure S18. ^{1}H (*top*) and 2D–DOSY (*bottom*) NMR spectra of macrocycle **6** in $CDCl_3$ at 25°C.

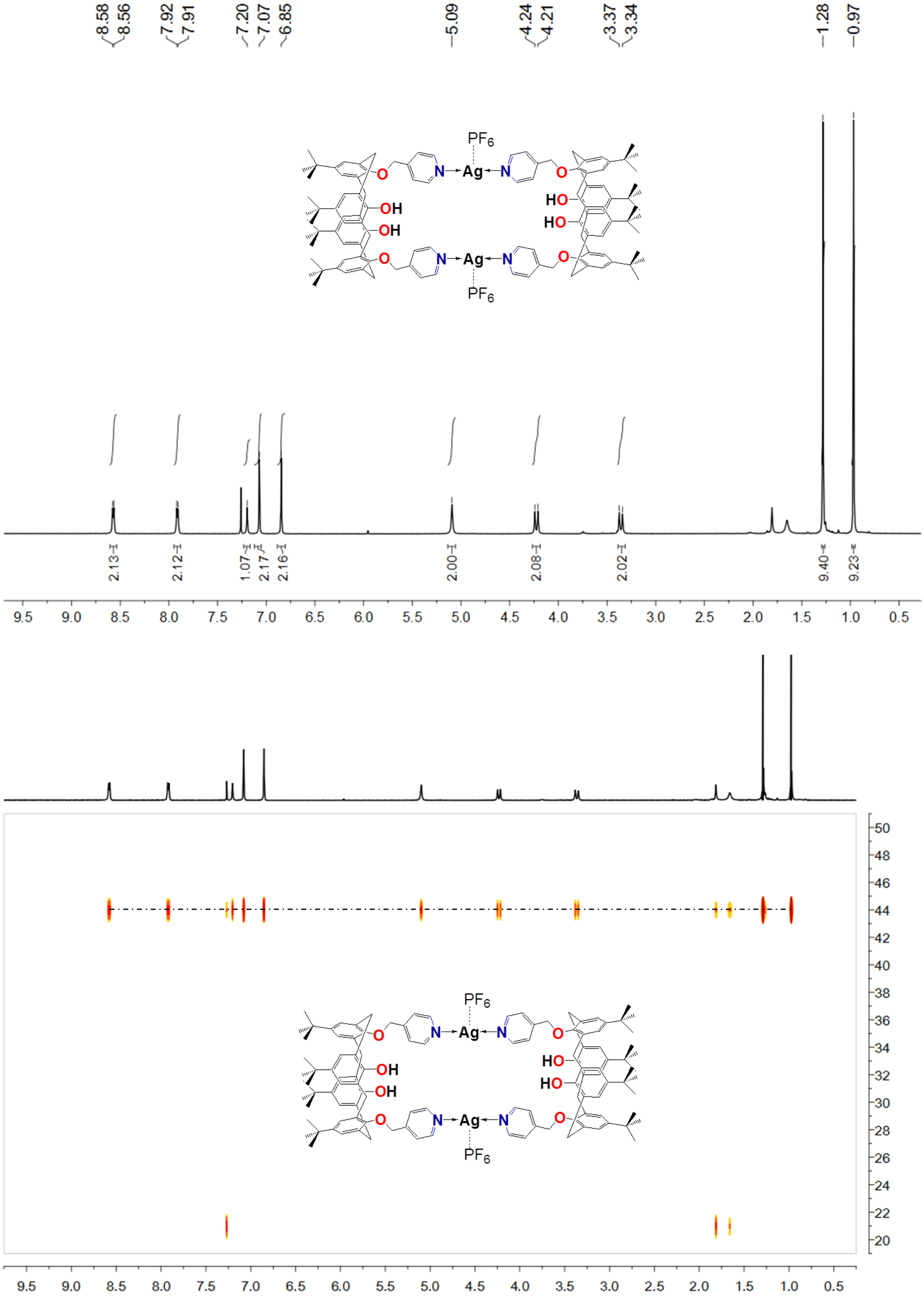

Figure S19. ^{1}H (*top*) and 2D–DOSY (*bottom*) NMR spectra of macrocycle **7** in $CDCl_3$ at 25°C.

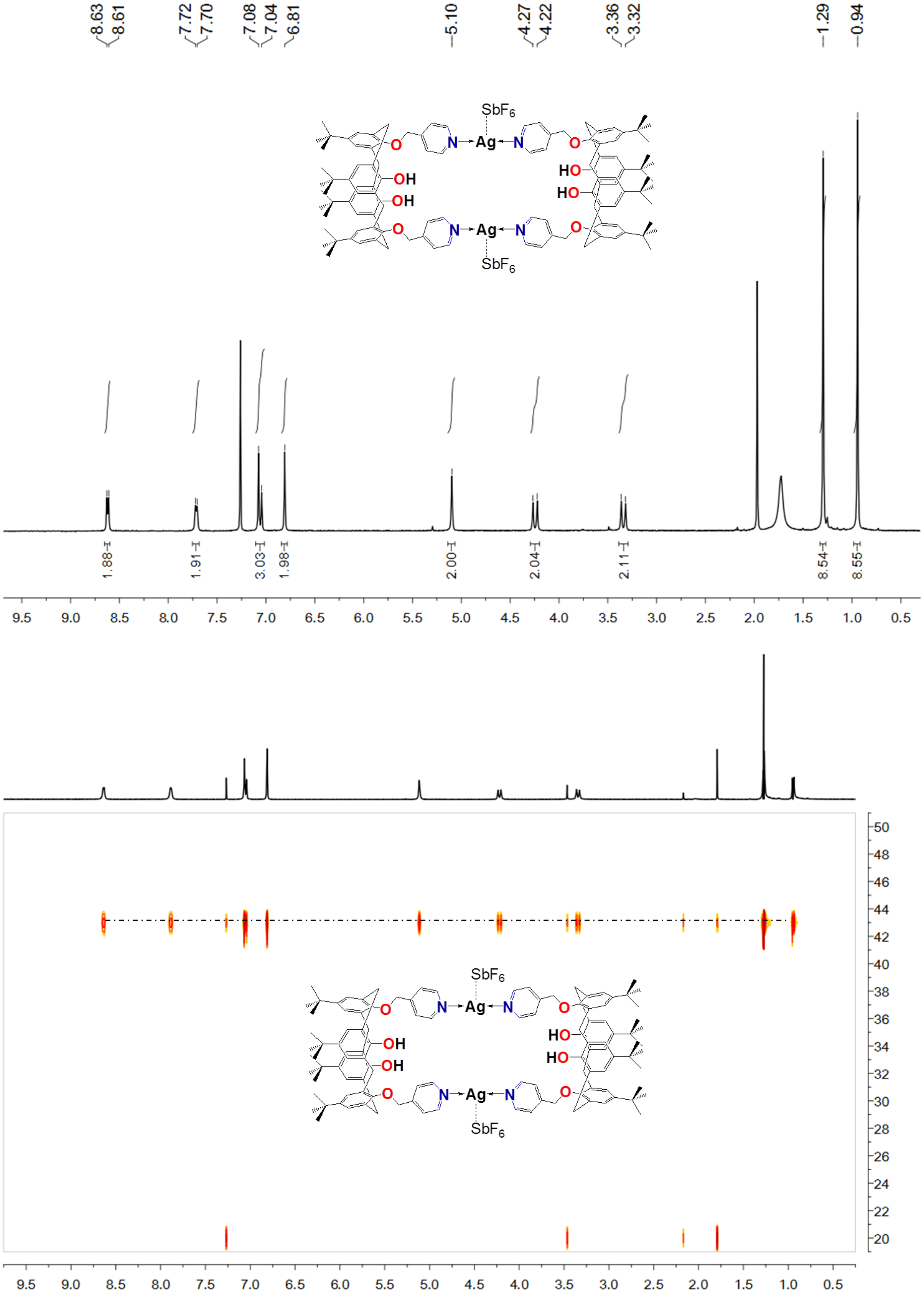

Figure S20. ^{1}H (*top*) and 2D–DOSY (*bottom*) NMR spectra of macrocycle **8** in $CDCl_3$ at 25°C.

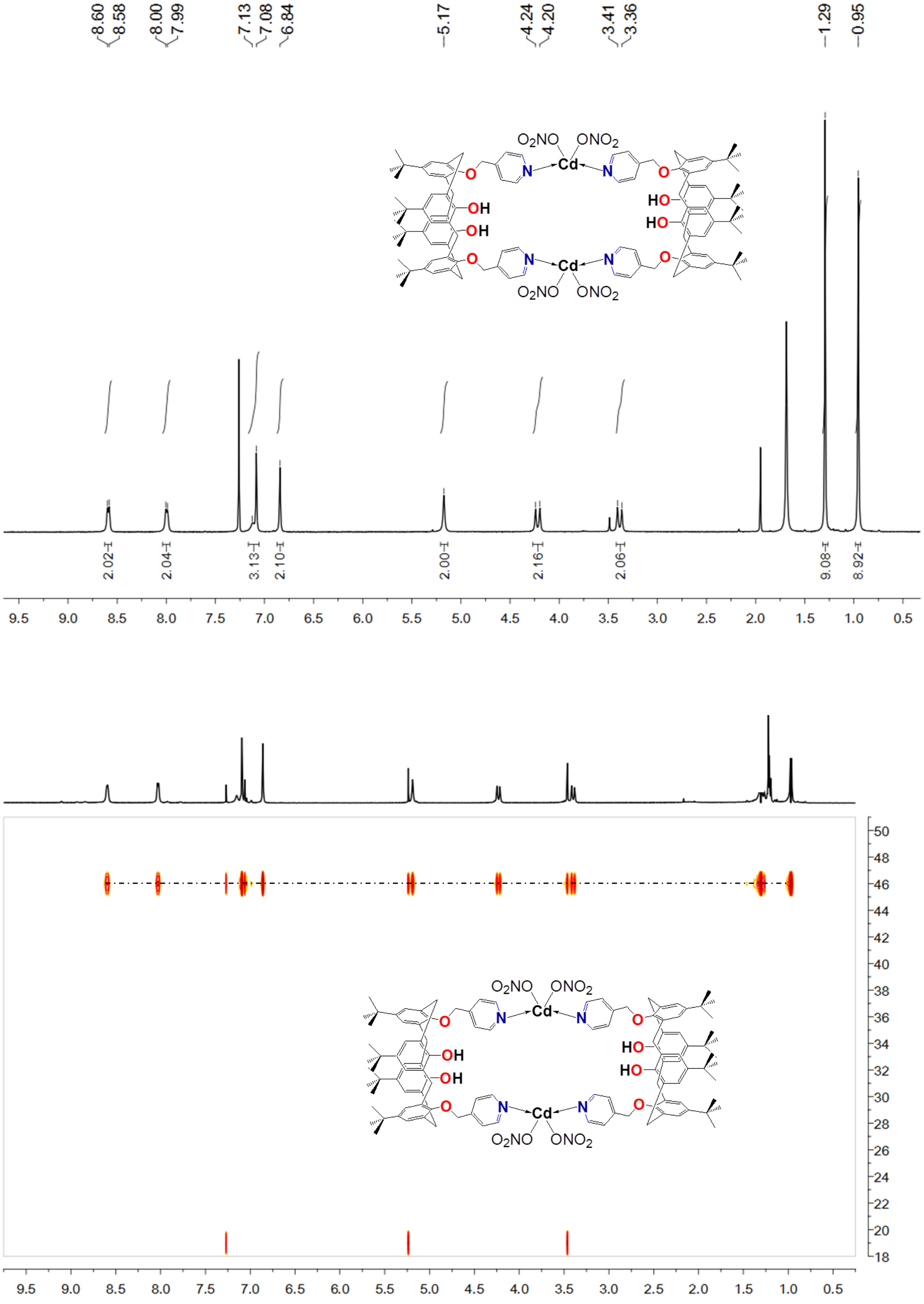

Figure S21. ^{1}H (*top*) and 2D–DOSY (*bottom*) NMR spectra of macrocycle **9** in $CDCl_3$ at 25°C.

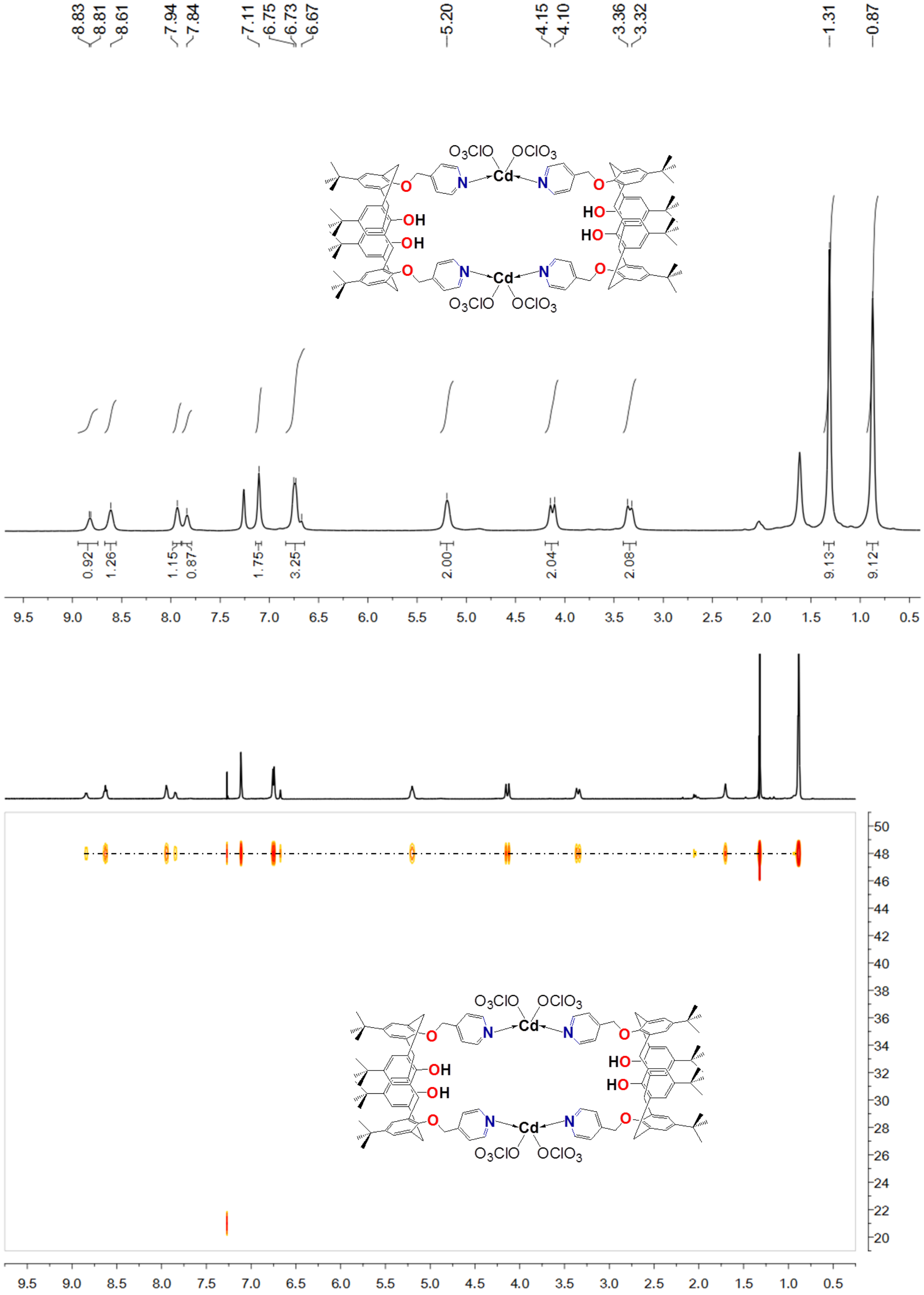

Figure S22. ^{1}H (*top*) and 2D–DOSY (*bottom*) NMR spectra of macrocycle **10** in $CDCl_3$ at 25°C.

4. ESI-MS

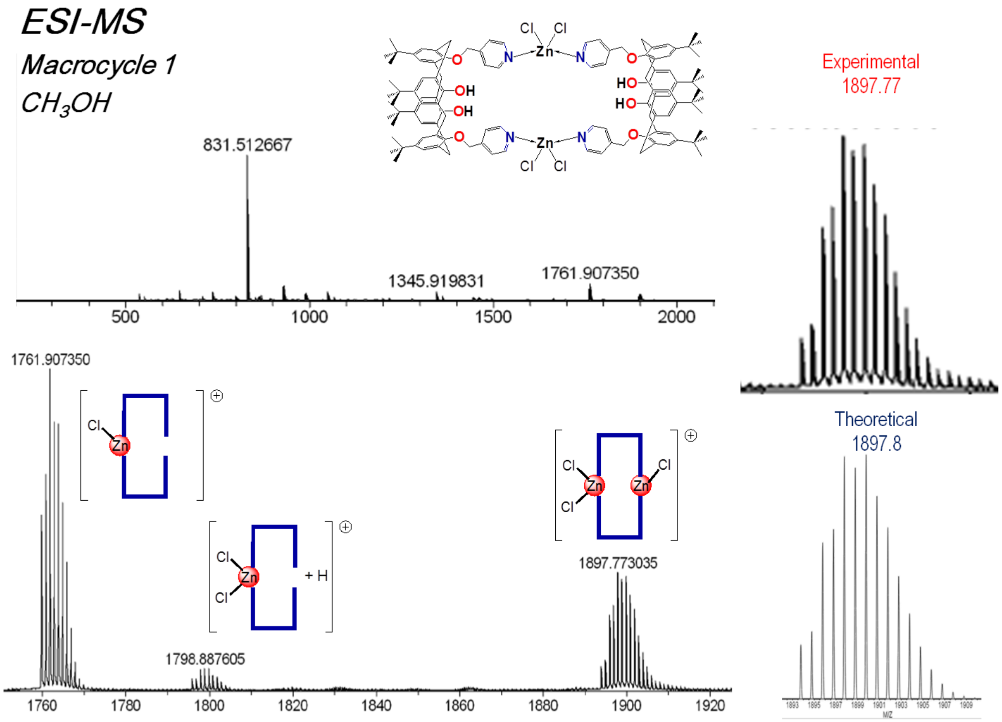

Figure S23. ESI-MS spectrum of macrocycle **1** including the experimental and theoretical isotopic patterns for **[$Zn_2L_2Cl_4$**–1Cl^-**]**$^+$ fragment.

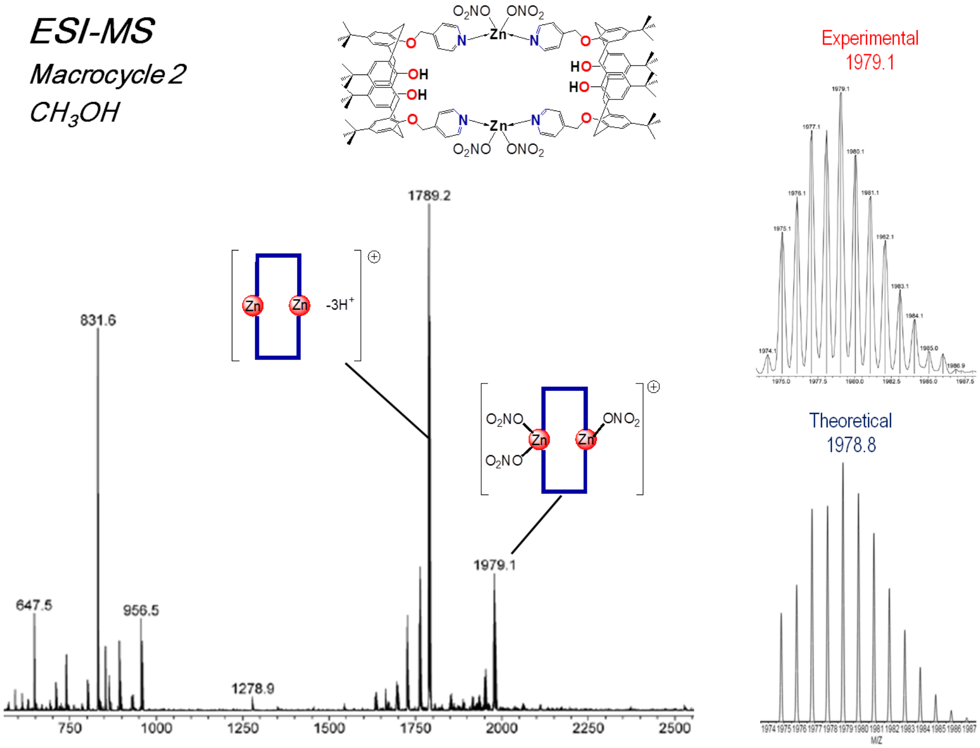

Figure S24. ESI-MS spectrum of macrocycle **2** including the experimental and theoretical isotopic patterns for **[$Zn_2L_2(NO_3)_4$**–1$(NO_3)^-$**]**$^+$ fragment.

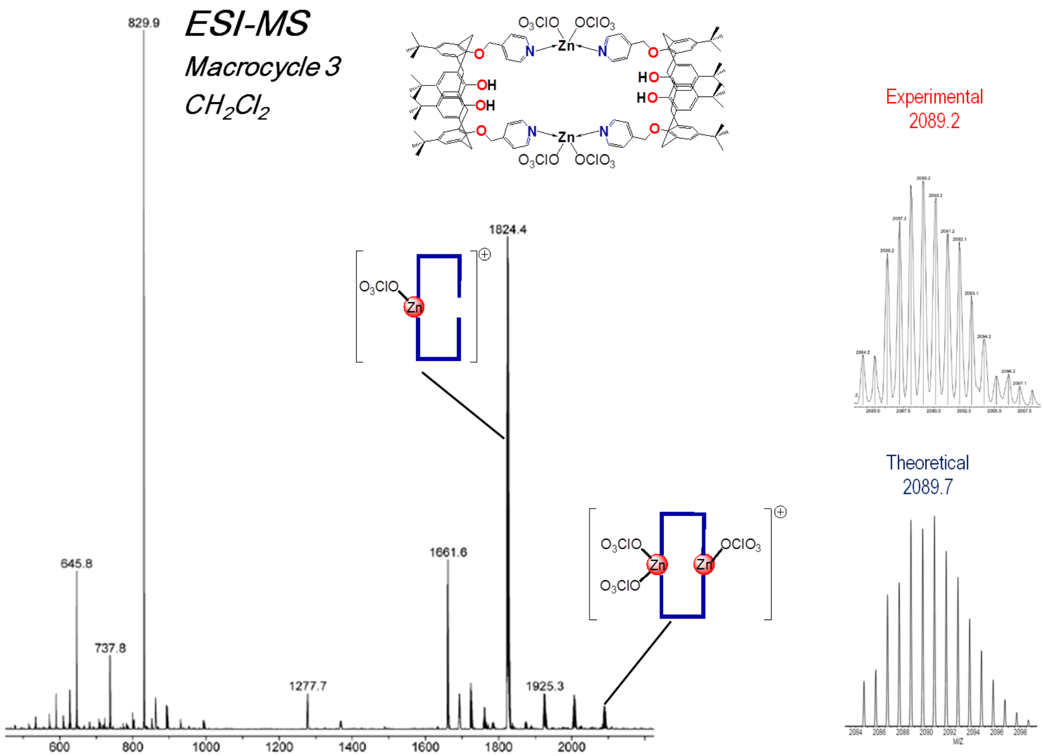

Figure S25. ESI-MS spectrum of macrocycle **3** including the experimental and theoretical isotopic patterns for $\mathbf{[Zn_2L_2(ClO_4)_4}-1(\mathrm{ClO_4})^{-}\mathbf{]}^{+}$ fragment.

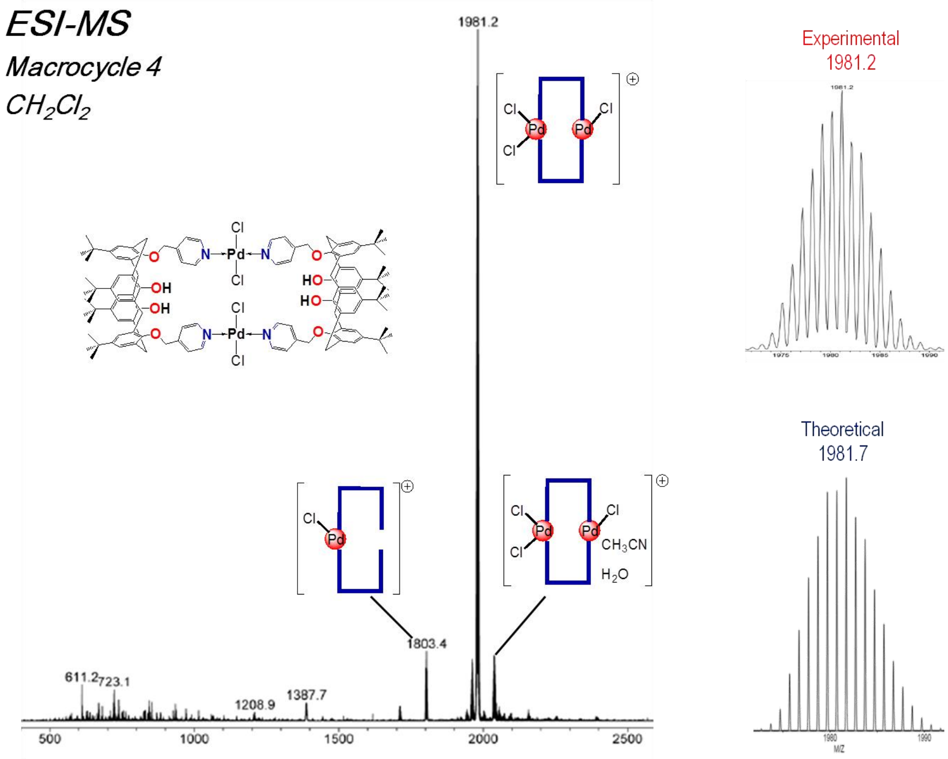

Figure S26. ESI-MS spectrum of macrocycle **4** including the experimental and theoretical isotopic patterns for $\mathbf{[Pd_2L_2Cl_4}-1\mathrm{Cl}^{-}\mathbf{]}^{+}$ fragment.

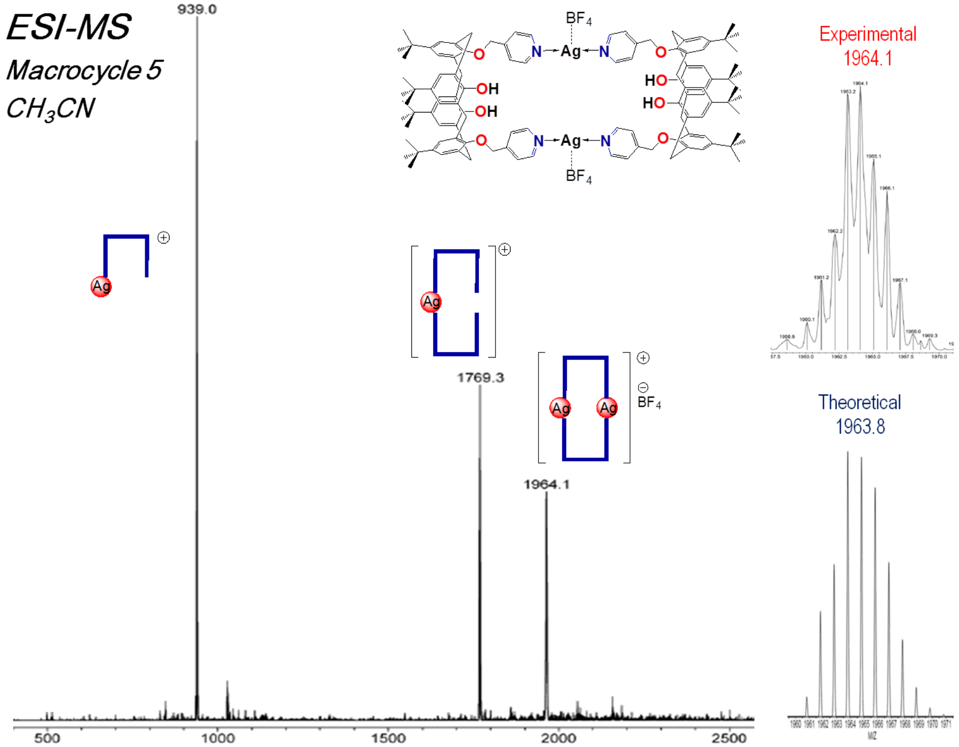

Figure S27. ESI-MS spectrum of macrocycle **5** including the experimental and theoretical isotopic patterns for **[Ag$_2$L$_2$(BF$_4$)$_2$**–1(BF$_4$)$^{-}$**]**$^{+}$ fragment.

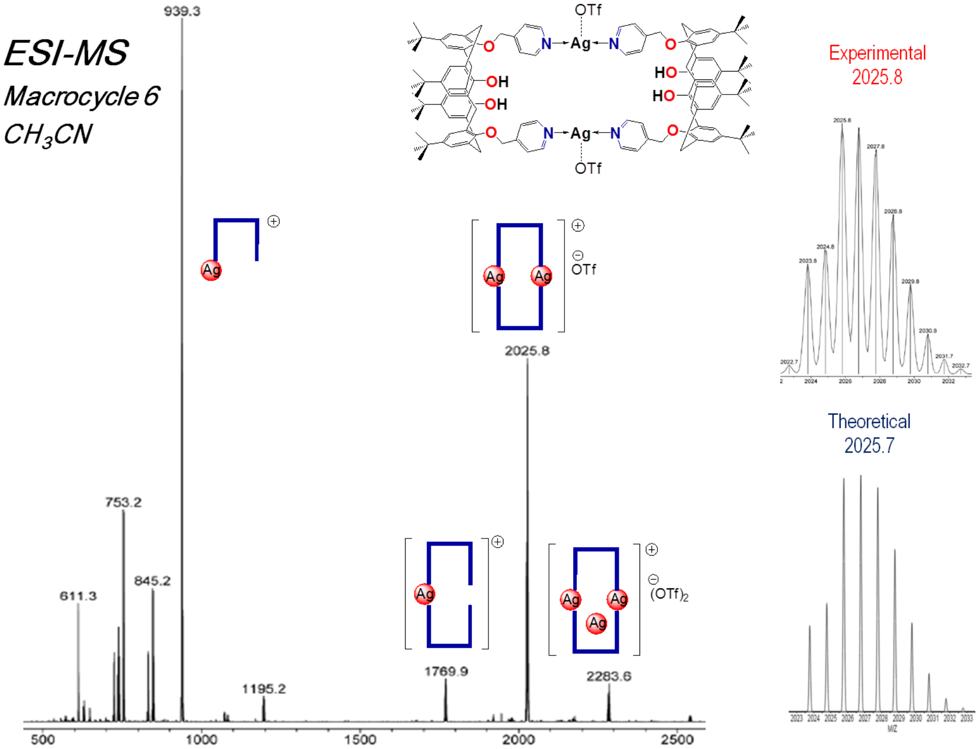

Figure S28. ESI-MS spectrum of macrocycle **6** including the experimental and theoretical isotopic patterns for **[Ag$_2$L$_2$(OTf)$_2$**–1(OTf)$^{-}$**]**$^{+}$ fragment.

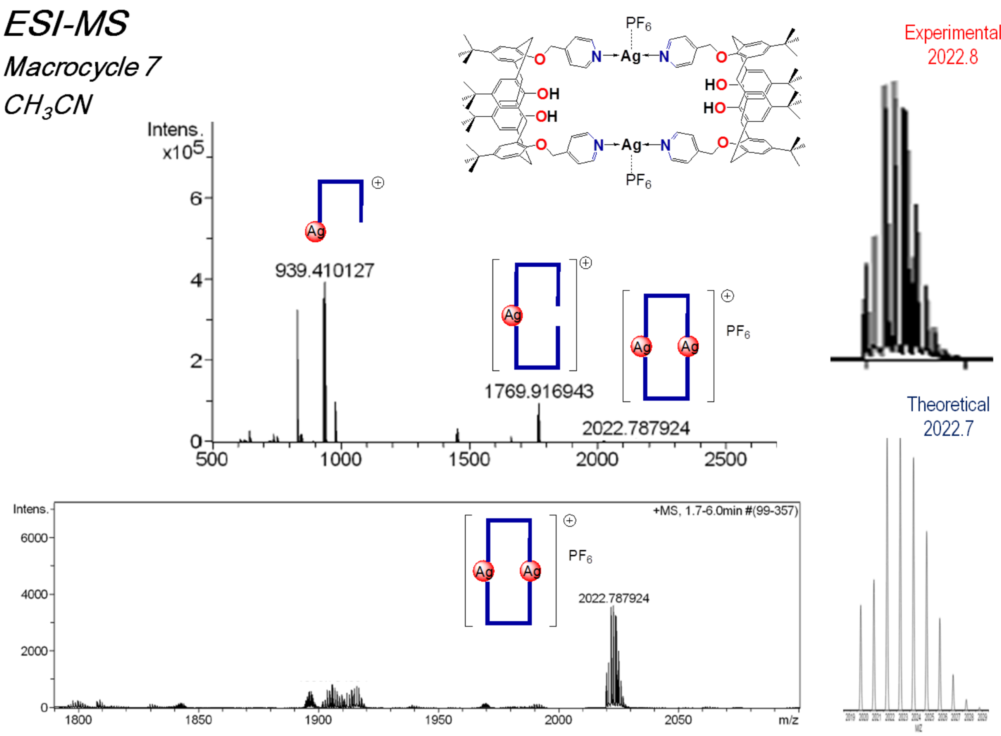

Figure S29. ESI-MS spectrum of macrocycle **7** including the experimental and theoretical isotopic patterns for **[Ag$_2$L$_2$(PF$_6$)$_2$**–1(PF$_6$)$^-$**]**$^+$ fragment.

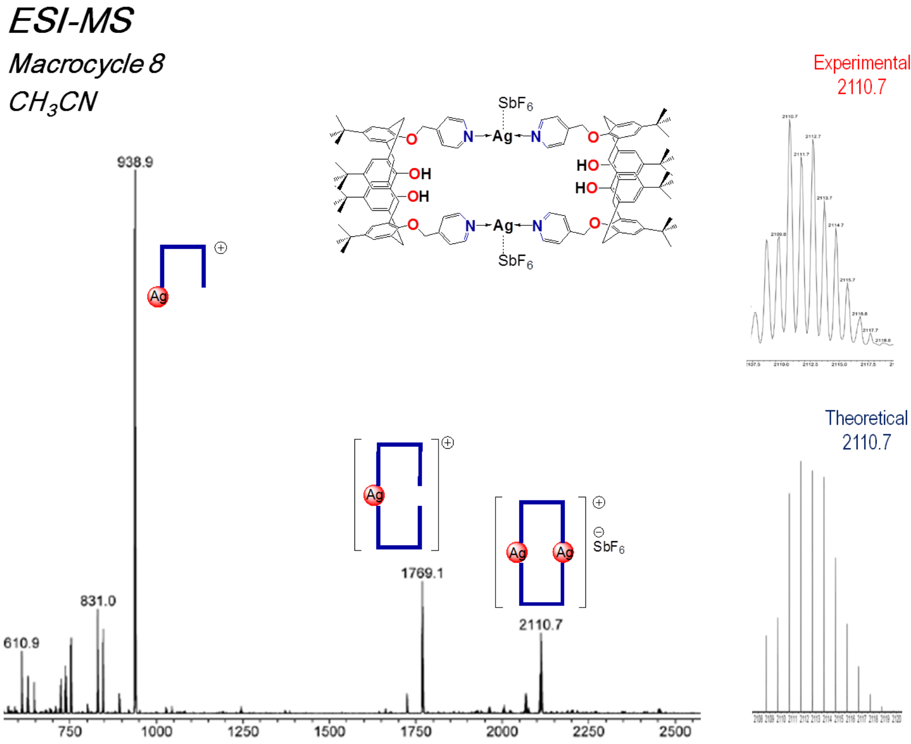

Figure S30. ESI-MS spectrum of macrocycle **8** including the experimental and theoretical isotopic patterns for **[Ag$_2$L$_2$(SbF$_6$)$_2$**–1(SbF$_6$)$^-$**]**$^+$ fragment.

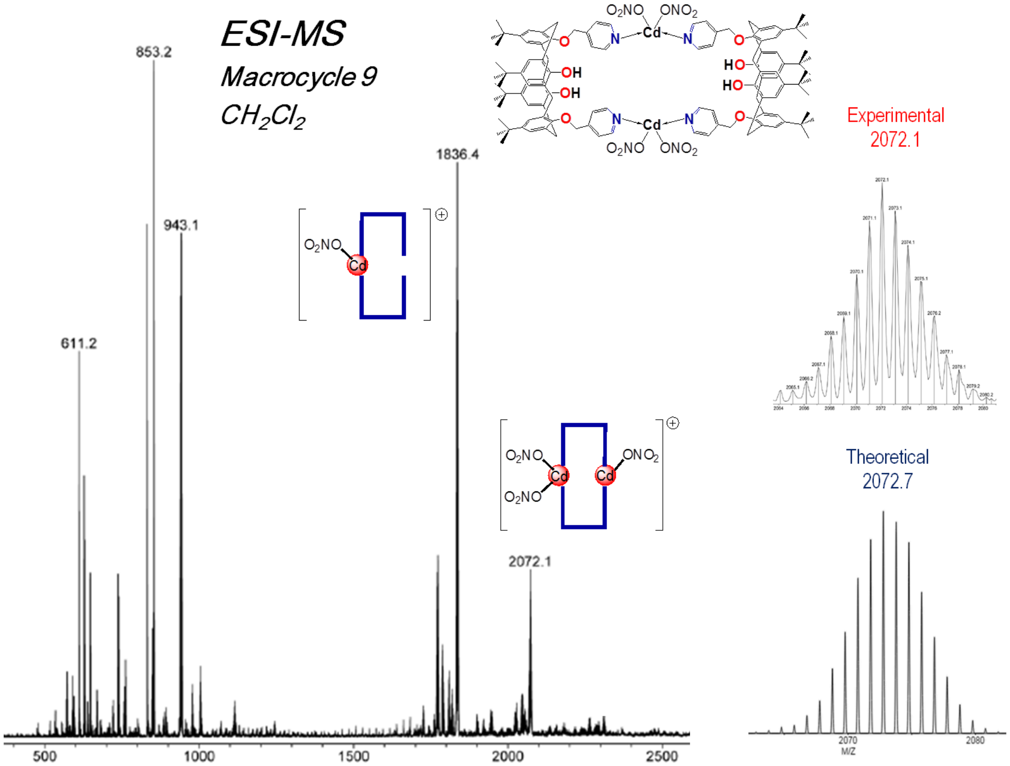

Figure S31. ESI-MS spectrum of macrocycle **9** including the experimental and theoretical isotopic patterns for **$[Cd_2L_2(NO_3)_4$**$–1(NO_3)^-$**$]^+$** fragment.

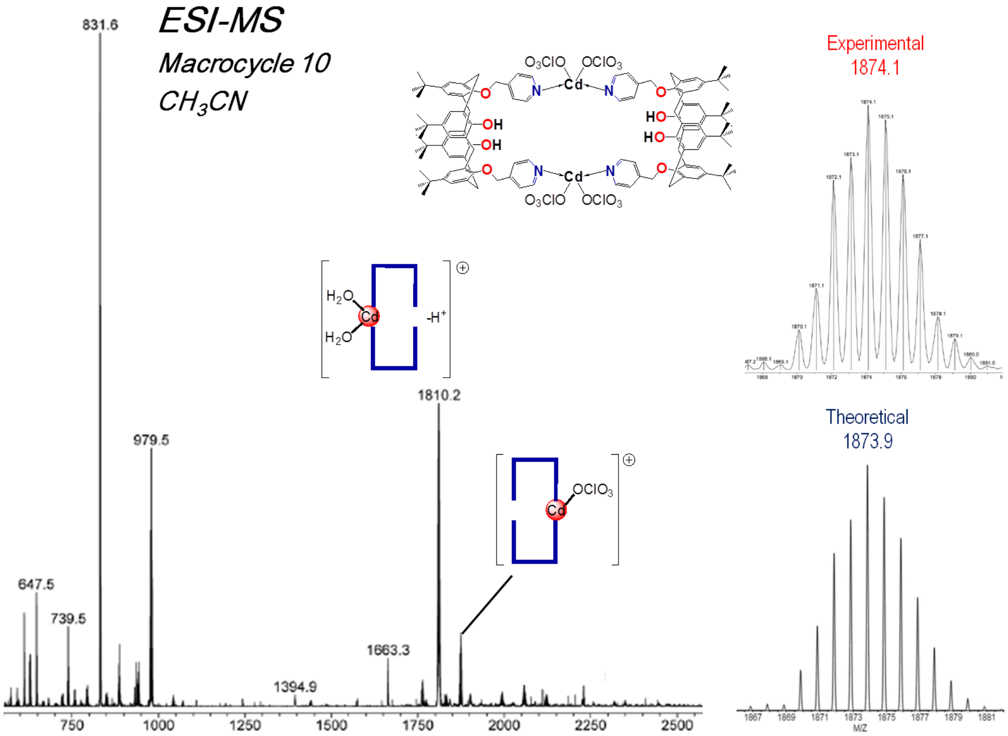

Figure S32. ESI-MS spectrum of macrocycle **10** including the experimental and theoretical isotopic patterns for **$[Cd_2L_2(ClO_4)_4$**$–1Cd(ClO_4)_2–1(ClO_4)^-$**$]^+$** fragment.

5. Absorption UV-Vis spectra and Fluorescence spectra in MeOH and $CHCl_3$.

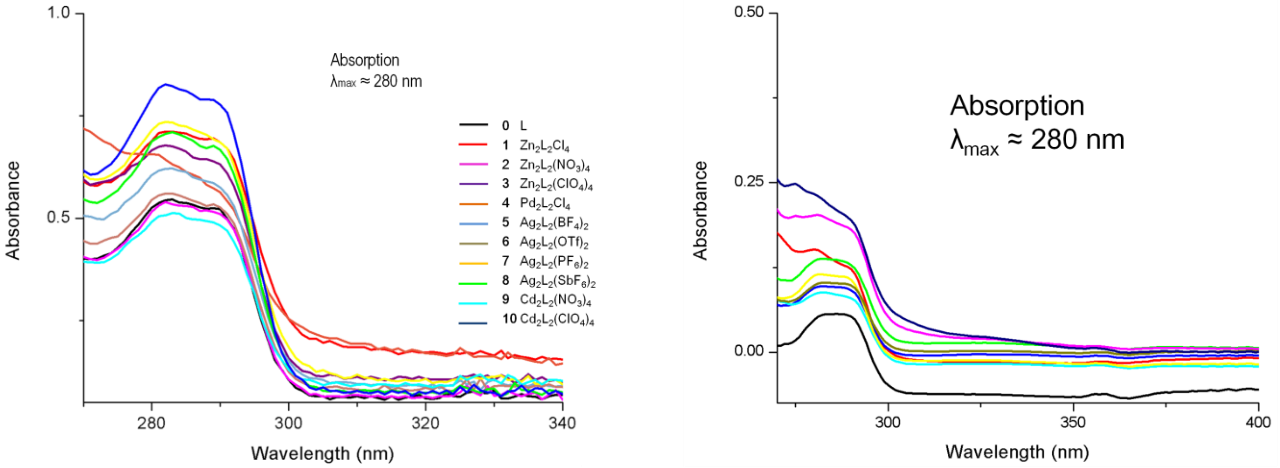

Figure S33. UV-Vis spectra of calix[4]arene **L** ($17x10^{-6}$ M) and macrocycles **1–10** ($8.5x10^{-6}$ M) recorded in MeOH (*left*) and $CHCl_3$ (*right*) at room temperature.

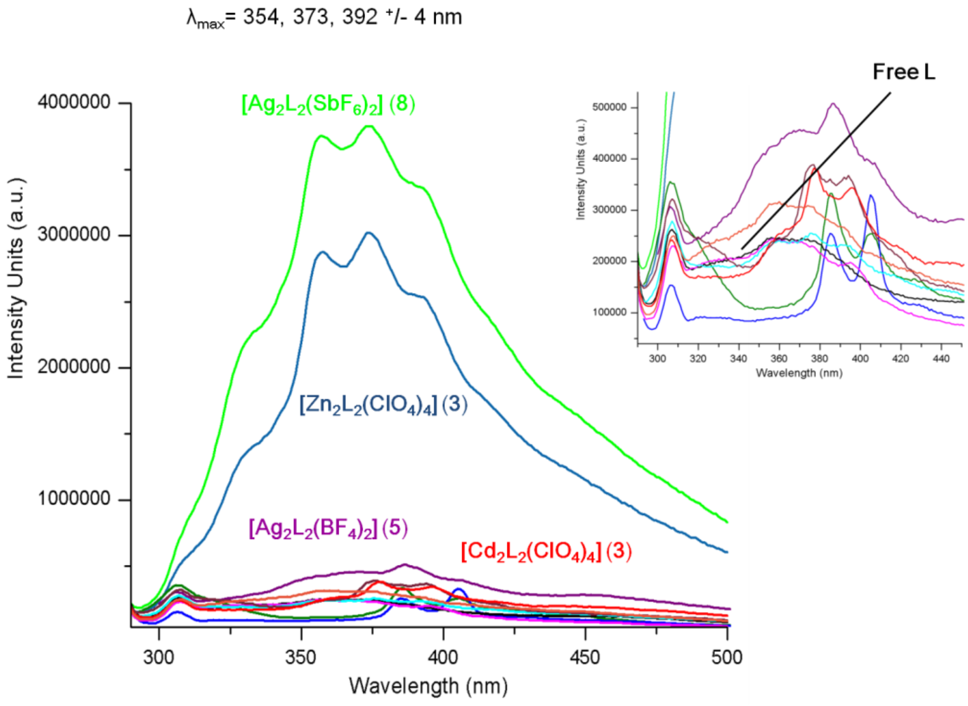

Figure S34. Florescence spectra of calix[4]arene **L** ($17x10^{-6}$ M) and macrocycles **1–10** ($8.5x10^{-6}$ M) recorded in $CHCl_3$ at room temperature.

6. Fluorescence "Turn-On" and "Turn-Off" titrations

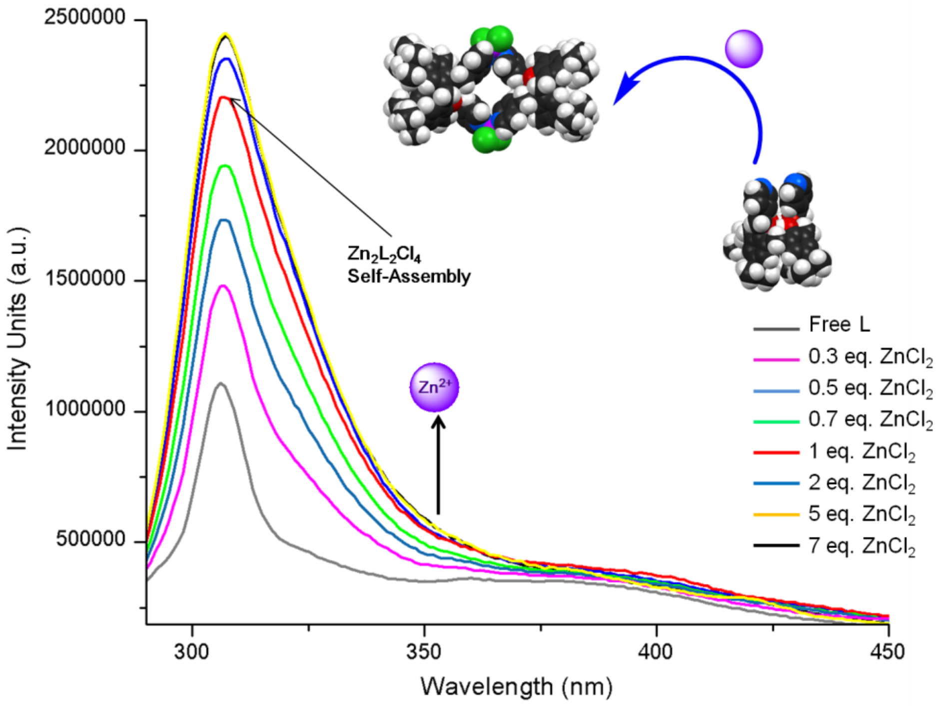

Figure S35. Enhancement of fluorescence of **L** ($8.5x10^{-6}$ M solution in MeOH) upon assembly of macrocycle **1**, and relative changes with addition of excess of $ZnCl_2$.

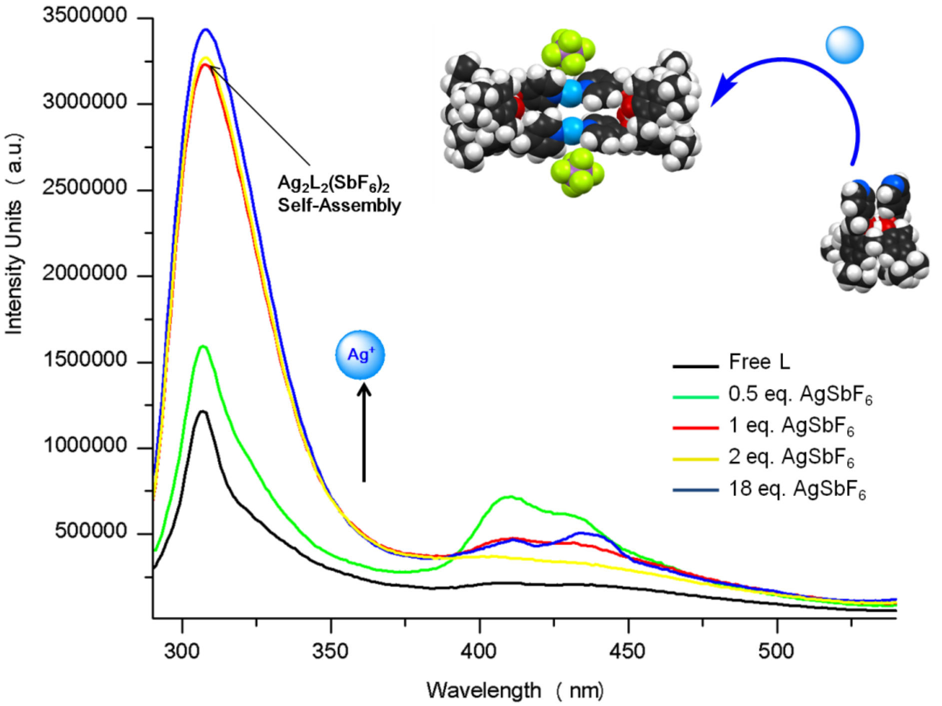

Figure S36. Enhancement of fluorescence of **L** ($8.5x10^{-6}$ M solution in MeOH) upon assembly of macrocycle **8**, and relative changes with addition of excess of $AgSbF_6$.

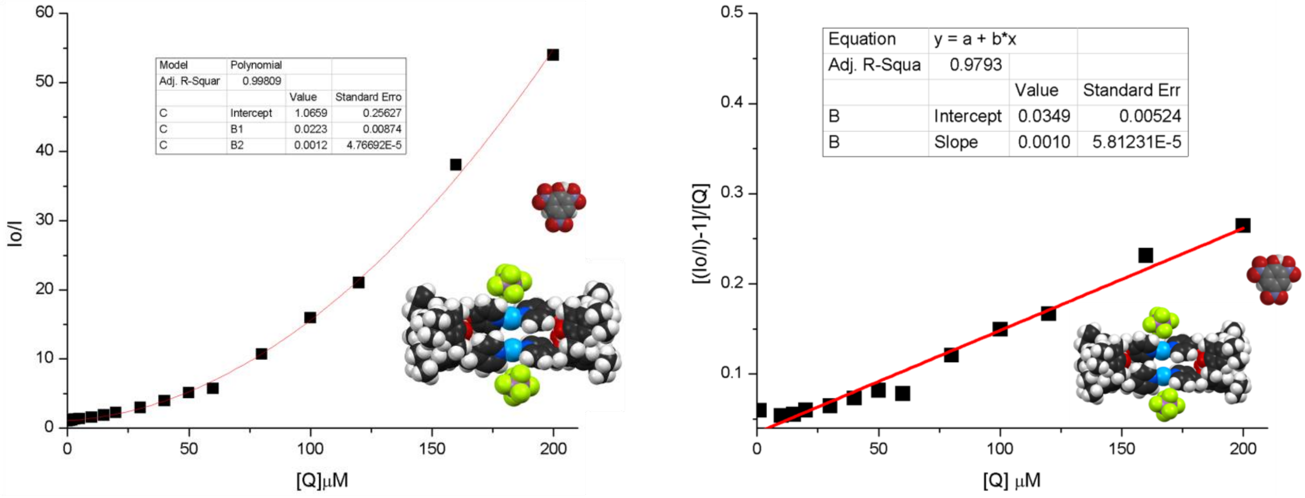

Model	Polynomial		
Adj. R-Squar	0.99809		
		Value	Standard Erro
C	Intercept	1.0659	0.25627
C	B1	0.0223	0.00874
C	B2	0.0012	4.76692E-5

Equation	y = a + b*x		
Adj. R-Squa	0.9793		
		Value	Standard Err
B	Intercept	0.0349	0.00524
B	Slope	0.0010	5.81231E-5

Figure S37. Stern-Volmer curve *Io/I* vs *[Q]* obtained from fluorescence quenching titration of macrocycle **8** ($8.5x10^{-6}$ M solution in $CHCl_3$) employing picric acid as quencher (*left*), and the corresponding modified Stern-Volmer plot [(*Io/I*)–1]/[*Q*] vs *[Q]* (*right*).

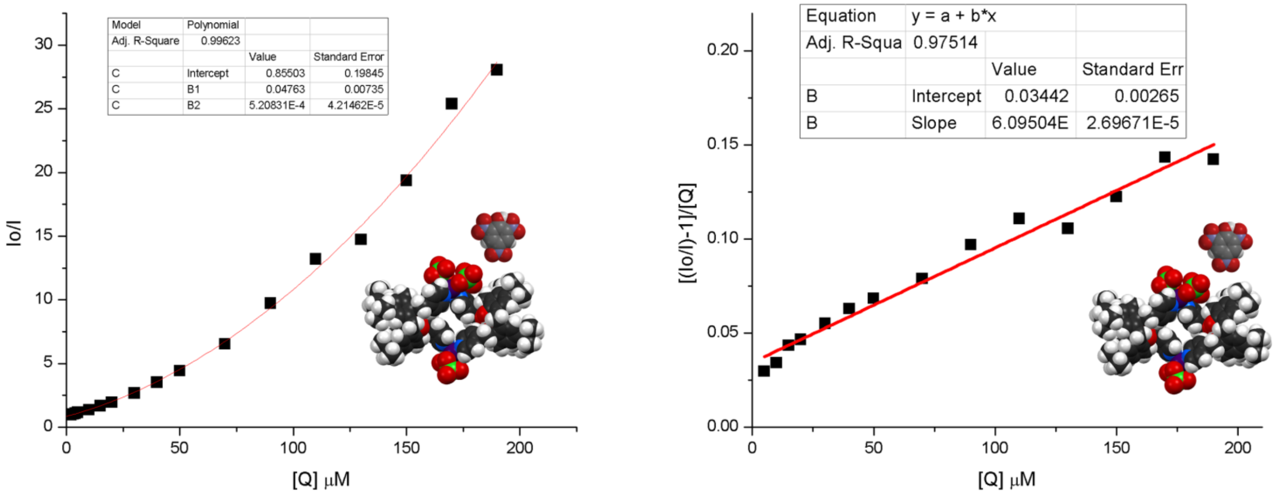

Model	Polynomial		
Adj. R-Square	0.99623		
		Value	Standard Error
C	Intercept	0.85503	0.19845
C	B1	0.04763	0.00735
C	B2	5.20831E-4	4.21462E-5

Equation	y = a + b*x		
Adj. R-Squa	0.97514		
		Value	Standard Err
B	Intercept	0.03442	0.00265
B	Slope	6.09504E	2.69671E-5

Figure S38. Stern-Volmer curve *Io/I* vs *[Q]* obtained from fluorescence quenching titration of macrocycle **10** ($8.5x10^{-6}$ M solution in $CHCl_3$) employing picric acid as quencher (*left*), and the corresponding modified Stern-Volmer plot [(*Io/I*)–1]/[*Q*] vs *[Q]* (*right*).

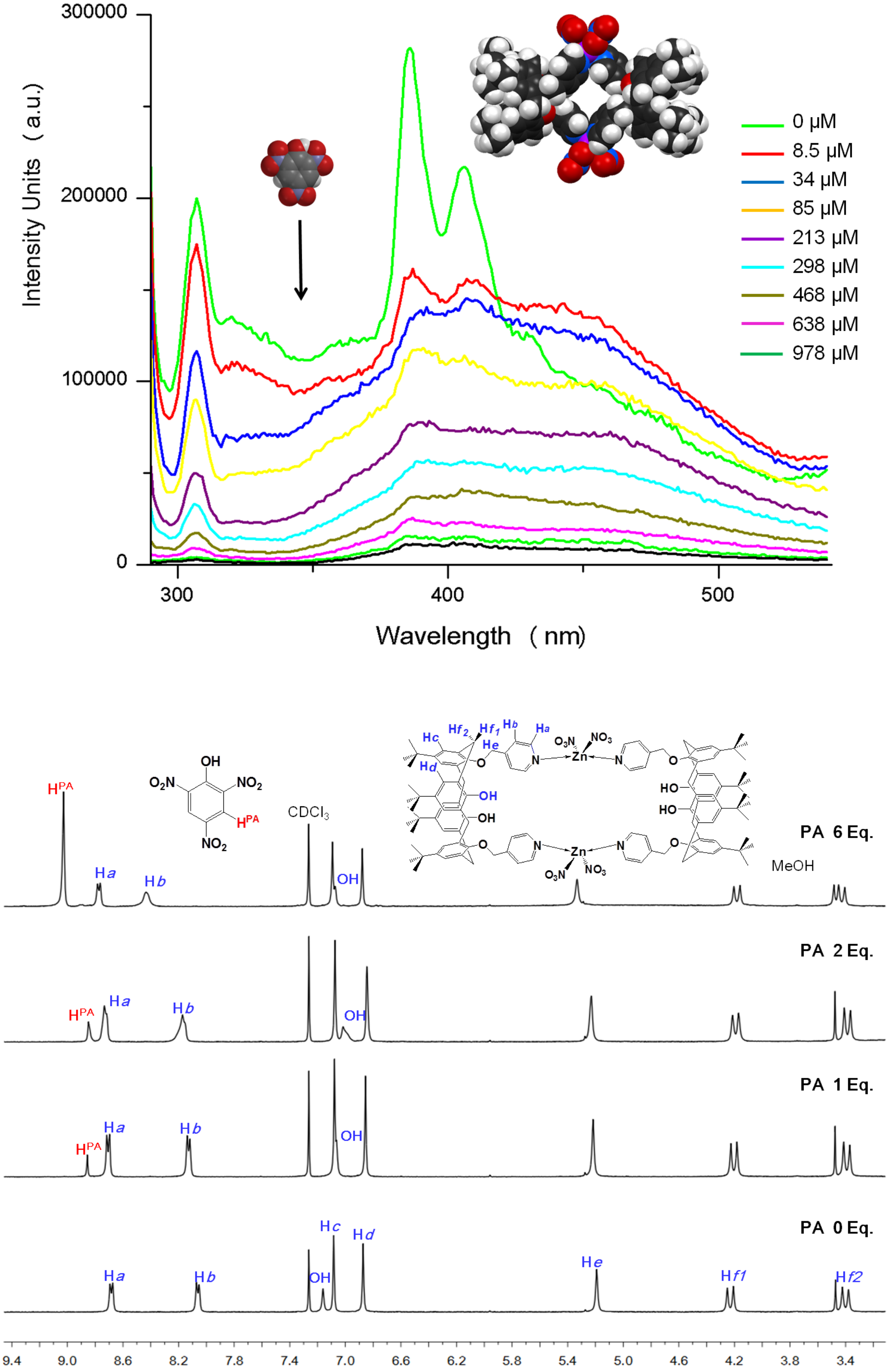

Figure S39. Fluorescence quenching profile of macrocycle **2** (8.5x10^{-6} M solution in CHCl$_3$) upon gradual addition of picric acid (*top*), and ^{1}H NMR titration plots in CDCl$_3$ (*bottom*).

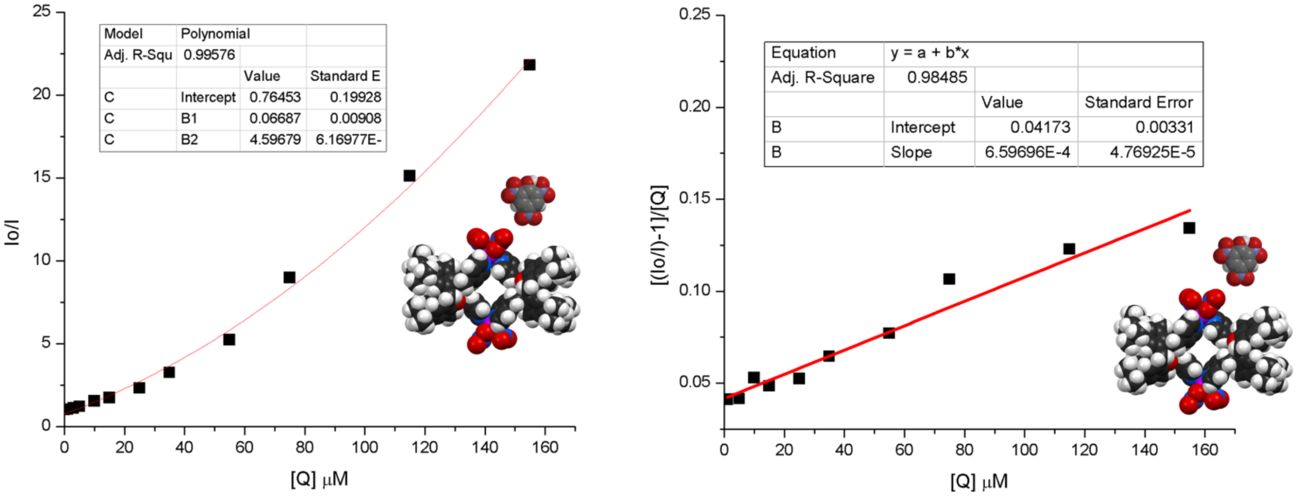

Model	Polynomial		
Adj. R-Squ	0.99576		
		Value	Standard E
C	Intercept	0.76453	0.19928
C	B1	0.06687	0.00908
C	B2	4.59679	6.16977E-

Equation	y = a + b*x		
Adj. R-Square	0.98485		
		Value	Standard Error
B	Intercept	0.04173	0.00331
B	Slope	6.59696E-4	4.76925E-5

Figure S40. Stern-Volmer curve *Io/I* vs *[Q]* obtained from fluorescence quenching titration of macrocycle **2** ($8.5\text{x}10^{-6}$ M solution in $CHCl_3$) employing picric acid as quencher (*left*), and the corresponding modified Stern-Volmer plot [(*Io/I*)–1]/[*Q*] vs *[Q]* (*right*).

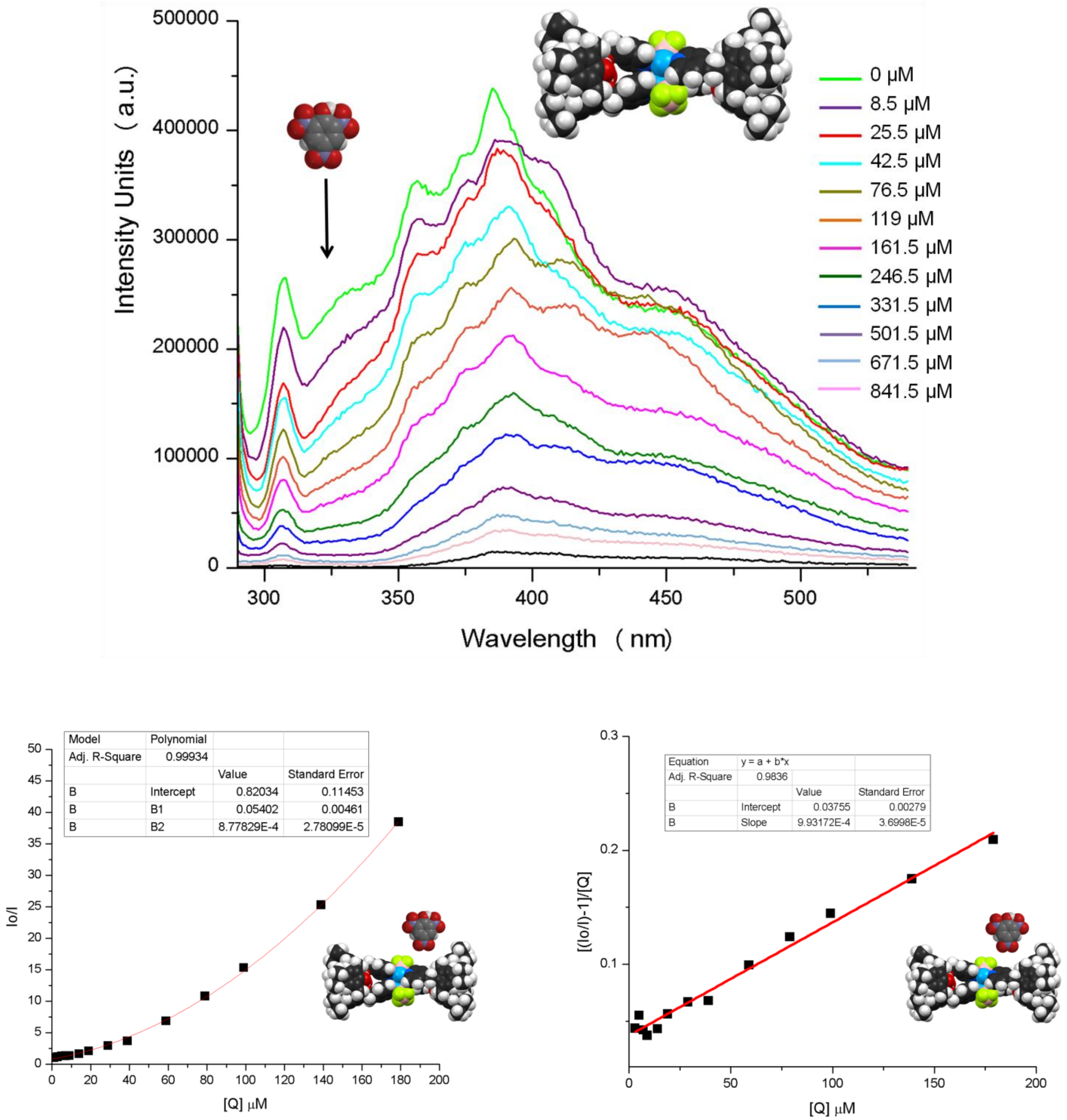

Model	Polynomial		
Adj. R-Square	0.99934		
		Value	Standard Error
B	Intercept	0.82034	0.11453
B	B1	0.05402	0.00461
B	B2	8.77829E-4	2.78099E-5

Equation	y = a + b*x		
Adj. R-Square	0.9836		
		Value	Standard Error
B	Intercept	0.03755	0.00279
B	Slope	9.93172E-4	3.6998E-5

Figure S41. Fluorescence quenching profile of macrocycle **5** (8.5×10^{-6} M solution in $CHCl_3$) upon gradual addition of picric acid (*top*), including the corresponding Stern-Volmer curve *Io/I* vs *[Q]* and the modified Stern-Volmer plot [(*Io/I*)–1]/[*Q*] vs *[Q]* (*bottom*).

7. X-ray Diffraction

Table S1. Collection data and refinement parameters for calixarene **L**.

	bis-Picolylcalix[4]arene [**L**•(dmso)$_2$]
Empirical formula	C60 H78 N2 O6 S2
Formula weight	987.36
Temperature	130(2) K
Wavelength	0.71073 Å
Crystal system	Triclinic
Space group	P –1
Unit cell dimensions	a = 11.5555(5) Å
	b = 13.2415(5) Å
	c = 20.8060(7) Å
	α = 94.145(3)
	β = 92.860(3)
	γ = 115.723(4)
Volume	2848.9(2) Å^3
Z	2
Density (calculated)	1.151 Mg/m^3
Absorption coefficient	0.143 mm^{-1}
F(000)	1064
Theta range for data collection	3.531 to 29.456°.
Index ranges	-11<=h<=15, -18<=k<=17, -27<=l<=28
Reflections collected	25879
Independent reflections	13289 [R(int) = 0.0454]
Completeness to theta = 25.242°	99.7 %
Refinement method	Full-matrix least-squares on F^2
Data / restraints / parameters	13289 / 14 / 670
Goodness-of-fit on F^2	1.054
Final R indices [I>2sigma(I)]	R1 = 0.0665, wR2 = 0.1603
R indices (all data)	R1 = 0.0906, wR2 = 0.1823
Largest diff. peak and hole	1.723 and -1.873 e.Å^{-3}

Table S2. Selected geometrical parameters of **L** accompanied by MERCURY representations of asymmetric unit and crystal packing of **L** with numbering.

	Bond length (Å)	Angles (°)	
C1–O1	1.392(2)	C1–O1–C45	113.71(15)
C12–O2	1.370(2)	O1–C45–C46	109.72(17)
C23–O3	1.395(2)	C48–N1–C49	116.1(2)
C34–O4	1.369(3)	C23–O3–C51	114.44(15)
C45–O1	1.430(2)	O3–C51–C52	109.63(17)
C51–O3	1.431(2)	C54–N2–C55	115.8(2)
C45–C46	1.502(3)		
C46–C47	1.386(3)		
C47–C48	1.388(3)		
C48–N1	1.333(3)		
C51–C52	1.501(3)		
C52–C53	1.387(3)		
C53–C54	1.384(3)		
C54–N2	1.335(3)